International Journal of Fatigue 115 (2018) 89–106

Contents lists available at ScienceDirect

International Journal of Fatigue

journal homepage: www.elsevier.com/locate/ijfatigue

Fatigue crack growth predictions based on damage accumulation ahead of the crack tip calculated by strip-yield procedures

Samuel Elias Ferreira*, Jaime Tupiassú Pinho de Castro, Marco Antonio Meggiolaro

Mechanical Engineering Department, PUC-Rio, Brazil

ARTICLE INFO

Keywords:
Fatigue crack growth models
Strip-yield mechanics
Fatigue crack closure
Effective stress intensity range
Damage accumulation ahead of the crack tip

ABSTRACT

Elber assumed a long time ago that ΔK_{eff} is the driving force for fatigue crack growth (FCG), and his hypothesis is the basis for strip-yield models widely used to predict residual lives of cracked components. However, this hypothesis cannot explain many load sequence effects observed in practice. Hence, it is at least worth to verify if FCG models based on ΔK_{eff} are indeed intrinsically better than concurrent models based on other principles. To do so, the same mechanics is used to predict FCG rates based both on Elber's ideas and on the alternative view that FCG is instead due to damage accumulation caused by the cyclic strain history ahead of the crack tip, an idea does not need or use the ΔK_{eff} hypothesis. To compare both approaches fairly, FCG rates are estimated by damage accumulation using the cyclic strain ranges induced by plastic displacements calculated by the very same procedures used by strip-yield models, assuming there are strain limits associated both with FCG thresholds and with material toughness. Despite based on apparently conflicting principles, both models can reproduce quite well FCG curves, a somewhat surprising result. Besides confirming that data fitting cannot be used to prove any model superiority, this result indicates that the ΔK_{eff} hypothesis is not a necessary requirement to explain the FCG behavior.

1. Introduction

Fatigue life predictions of cracked structural components are required in most design and/or structural integrity evaluation tasks. Since Paris and Erdogan clearly demonstrated that stable fatigue crack growth (FCG) rates da/dN correlate well with stress intensity factor (SIF) ranges ΔK [1], many similar rules have been proposed to consider effects of other parameters that can affect FCG rates as well, such as the peak load K_{max} or the load ratio $R = K_{min}/K_{max}$, as well as the material limits for da/dN, namely FCG thresholds $\Delta K_{th}(R)$ and the critical SIF K_{IC} or K_C [2]. Another important issue for FCG modeling came after Elber experimentally found the crack closure phenomenon [3]. He observed that fatigue cracks can partially close over the lower portion of their load cycles even under $R > 0$, and only completely open after the applied SIF exceeded the so-called crack opening load K_{op}. Moreover, from this observation, he then assumed that FCG can only occur only after the crack tip is fully open under loads greater than K_{op} (supposing that only then they would become able to expose their tips to additional fatigue damage) [4]. Consequently, he postulated that ΔK_{eff} ($\Delta K_{eff} = K_{max} - K_{op}$ if $K_{op} > K_{min}$, or $\Delta K_{eff} = \Delta K$ otherwise) would be the actual FCG driving force (instead of SIF ranges ΔK or SIF combinations like $\{\Delta K, K_{max}\}$ or $\{\Delta K, R\}$).

Since the ΔK_{eff} *hypothesis* can reasonably explain many (but certainly not all) sequence or load-order effects in FCG, like crack growth delays or arrests after overloads (OL) and the R-sensitivity of FCG thresholds (in non-inert environments), it has been popular among fatigue experts ever since its proposal. It has been used as the basis for many semi-empirical FCG models, in particular the so-called strip-yield models (SYM) that numerically estimate K_{op} and ΔK_{eff}, and from them FCG lives using a suitable $da/dN = f(\Delta K_{eff})$ equation properly fitted to experimental data [5–9]. However, although the fatigue crack closure phenomenon is well documented and proven [10–13], its real significance for FCG is still controversial, to say the least. Indeed, the ΔK_{eff} hypothesis cannot explain many FCG peculiarities, see for instance [14–19] for an overview of them.

An alternative and probably more intuitive and less controversial way to model FCG is to assume fatigue cracks grow by sequentially breaking small volume elements ahead of the crack tip, as they reach all the damage they can sustain due to the cyclic elastoplastic stress/strain histories that load them during their lives. In other words, these so-called critical damage models (CDM) suppose the crack increments are caused by the sequential rupture of small volume elements adjacent to their tips, which break after reaching the critical fatigue damage the material can endure [17,20–26].

* Corresponding author.
E-mail address: ferreirase@hotmail.com (S.E. Ferreira).

https://doi.org/10.1016/j.ijfatigue.2018.03.001
Received 12 October 2017; Received in revised form 13 January 2018; Accepted 1 March 2018
Available online 02 March 2018

A first comparative analysis between a simple CDM proposed in [24] and a classic SYM based on Newman's original formulation [6] has been recently presented in [27]. However, due to the lack of limit properties in the traditional εN procedures employed to calculate fatigue damage ahead of the crack tip, the CDM studied in [27] needs to use a McEvily-like FCG rule to properly consider the phase I and III behaviors of typical $da/dN \times \Delta K$ curves, using FCG thresholds ΔK_{th}(R) and toughnesses K_C to limit the estimated $da/dN \times \Delta K$ curves [24,26,27]. The main objective of this work is to propose an improvement to that model to eliminate the need for assuming and using such a reasonable albeit somehow arbitrary FCG rule. The new CDM proposed here directly estimates the entire $da/dN \times \Delta K$ behavior from simple and clear mechanical principles using only well-defined εN properties, without the need for any additional data-fitting parameter.

2. The ΔK_{eff} hypothesis

Elber identified crack closure almost 50 years ago by measuring compliance variations in a fatigue-cracked plate [3]. His measurements clearly indicate that a SIF $K_{op} > 0$ may be needed to completely open a fatigue crack. He imputed this phenomenon to tensile residual plastic strains that are always left around the crack faces on the wake of a fatigue crack, whose faces may thus remain under compression when unloaded. This contribution was important for understanding some peculiarities of the FCG behavior, and nowadays there is no serious doubt about the existence of crack closure. Indeed, it is well known that fatigue cracks open and close gradually, as it can be directly verified by Williams' et al. photographs reproduced in Fig. 1 [13], which clearly depict the gradual opening and closing of a fatigue crack during a load cycle.

Even though there is no reasonable doubt about the existence of fatigue crack closure, the same cannot be said about its actual significance for FCG. Elber *assumed* in 1971 that fatigue cracks cannot grow while their tips are partially closed [4], thus *supposing* that the portion of their load cycles with $K < K_{op}$ could not induce any further fatigue damage. Hence, he *postulated* that the actual FCG driving force would be ΔK_{eff}. To justify his claim, Elber fitted FCG da/dN data measured under constant ΔK in 2024-T3 Al alloy specimens by Forman, Paris-Erdogan and by his $da/dN = C\Delta K_{eff}^{m}$ rule, obtaining *rms* errors of 28, 27 and 21, respectively. The (slightly) better performance of his model was then used to sustain his *hypothesis* that ΔK_{eff} would be the actual FCG driving force (instead of the pairs $\{\Delta K, R\}$ or $\{\Delta K, K_{max}\}$ used by Forman, e.g.), although data fitting by no means can be assumed, let alone be used as a scientific proof, especially with such similar errors [28].

However, ΔK_{eff} concepts can indeed explain, at least in a qualitative way, many memory effects induced by variable amplitude loads (VAL). Moreover, since K_{op} can be measured by Elber's and by other reliable techniques, ΔK_{eff} predictions can and should be experimentally verified. Anyway, the key point behind the ΔK_{eff} *hypothesis* is that the material ahead of the crack tip cannot suffer any further fatigue damage below K_{op}, either during loading or unloading, because crack closure would completely shield the fatigue crack tip from additional strains. Fig. 2 schematizes the deformations expected in a point near the crack tip under a $P_{min} \rightarrow P_{max} \rightarrow P_{min} > 0$ load cycle, when there is no closure. An elastic behavior A → B is expected during the initial loading stretch, and it should be followed by plasticity at higher loads in the stretch B → C, see Fig. 2a. Likewise, elastic unloading is expected in the stretch C → D, after which the stresses inside the monotonic plastic zone pz ahead of the crack tip reach the compressive yield strength of the material, initiating the formation of the reverse plastic zone pz_r until the final unloading point E.

If crack closure can indeed totally shield the crack tip, as proposed by Elber, during the loading stretch it could not allow any deformation ahead of the crack tip until the load reaches the opening load P_{op}, see Fig. 2b. The inverse should occur during unloading, so the deformation should stop after the crack closure point (for simplicity considered equal to the opening point in the figure). However, if a strain cycle measured in a point ahead of the crack tip is closer to Fig. 2a than to Fig. 2b, crack closure would not totally shield the crack as proposed by Elber, since this load cycle portion below P_{op} would contribute to its fatigue damage (which is proportional to the strain range $\Delta\varepsilon$). This is especially important during unloading, when the reverse plastic zone is forming.

In view of that, Elber's own results, reproduced in Fig. 3 [4], can be used to question his ΔK_{eff} *hypothesis*. Fig. 3 shows the applied stress versus the displacement before, during, and after an OL, measured by a clip gage mounted ahead of the crack tip. The circles represent the

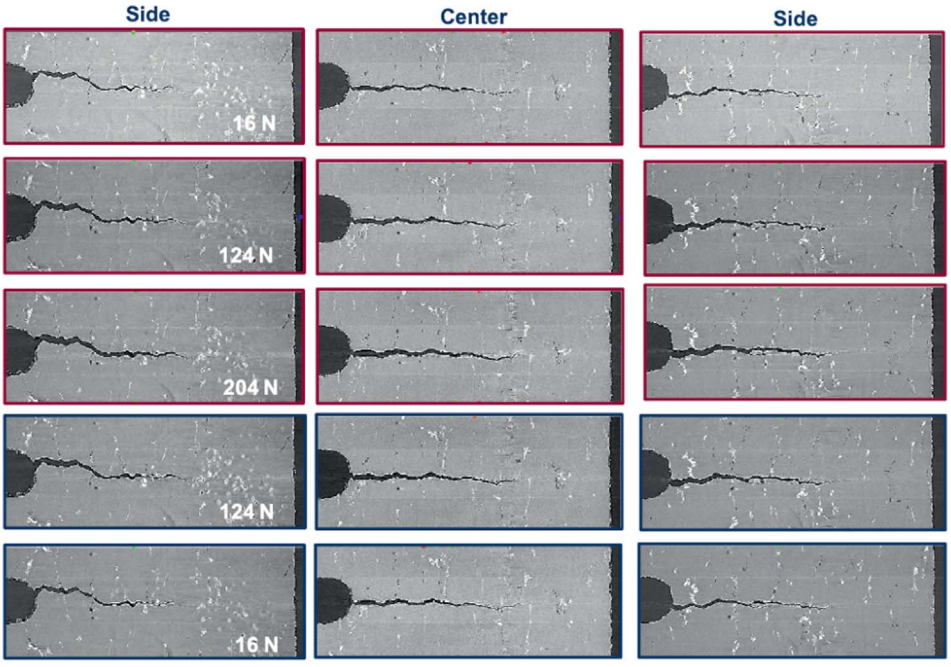

Fig. 1. The gradual opening and closing of a fatigue crack during a tensile load cycle [13].

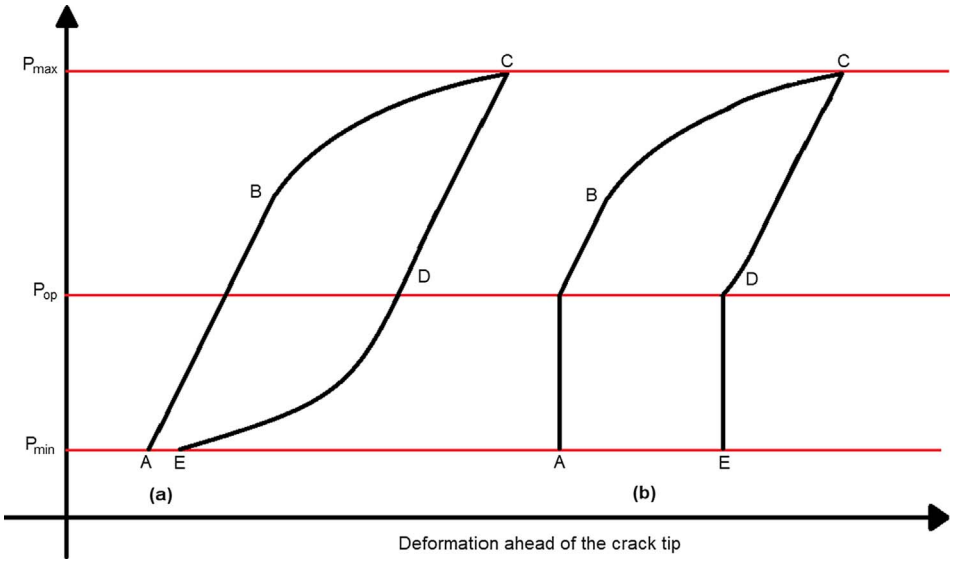

Fig. 2. Schematic behavior ahead of the crack tip: (a) no crack tip shielding, (b) crack tip completely shielded in the stretch $P_{min} \rightarrow P_{op}$, before and after the crack tip closes.

crack opening point. It is clear that the material ahead of the crack tip displaces below the opening load, both during the loading and the unloading portions of the load cycle. Consequently, that material is strained below K_{op}, so it is not completely shielded after the crack tip closes.

3. A few examples of data that question the actual ΔK_{eff} role in fatigue crack growth

James and Knott [29] investigated the intrinsic threshold SIF range of a quenched and tempered Q1N steel, measuring crack-opening loads and FCG rates in four-point bend specimens. They used an electro-discharge machine (EDM) to remove part of the plastic wake around the crack faces, to examine the effect of load shedding and load increasing testing schemes on the extent of crack closure. After reaching the threshold in an $R = 0.35$ test, they identified 1.2 mm of wake-induced closure. Part of this wake was removed by EDM, leaving only 0.5 mm of wake behind the crack tip. Upon restarting the test at the same load, they found that the growth rate was higher and the closure lower than during previous cycling, see Fig. 4.

The increase in FCG rates after the plastic wake removal is a clear evidence of how crack closure can affect them, but the authors unfortunately did not show if such rates increased as predicted by ΔK_{eff}. This is a most important point, because even when crack closure exists and can affect FCG rates, the question is whether its magnitude has the effect assumed when using ΔK_{eff} to model it.

That is why a small but representative set of results is presented following to discuss the actual ΔK_{eff} role in FCG. Countless authors tested Elber's hypothesis, but most of them just to reaffirm his idea, instead of to verify and understand the real influence of crack closure on FCG. For example, von Euw et al. [30] tested 2024-T3 Al 3.2 mm thick specimens to analyze OL effects on FCG rates, using Elber's $da/dN = C[(0.5 + 0.4R)\Delta K]^n$ empirical equation to estimate ΔK_{eff} [4]. They concluded ΔK_{eff} was the FCG driving force due to its reasonable correlation with their da/dN data. However, since a reasonable data-fitting performance cannot constitute a scientific proof, this conclusion

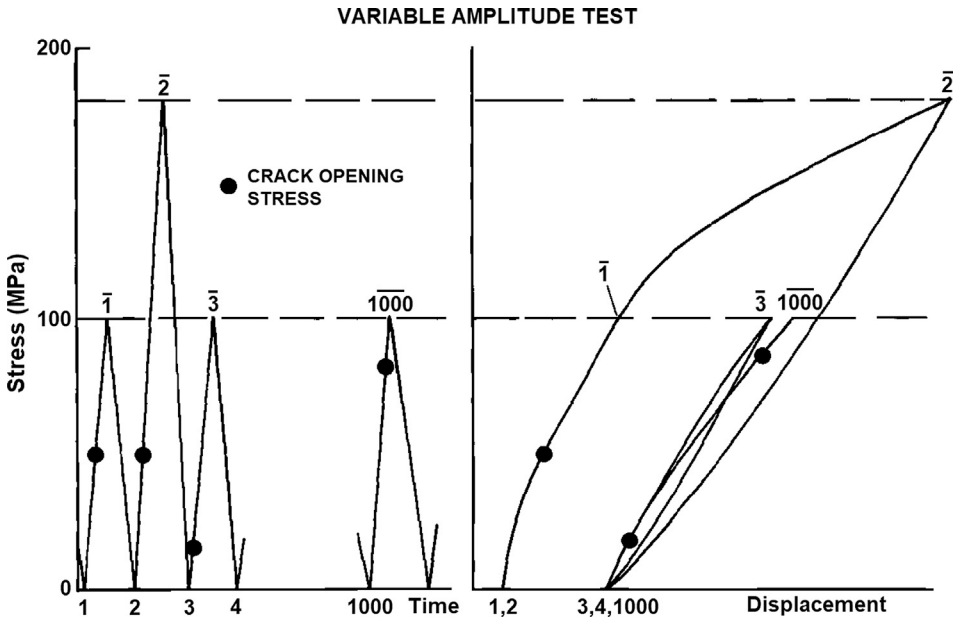

Fig. 3. Crack opening stress and displacements ahead of the crack tip [4].

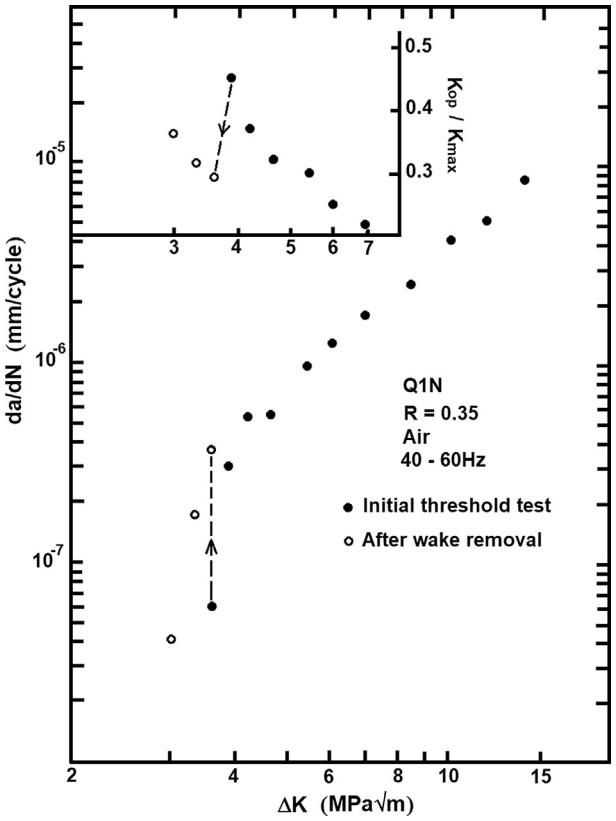

Fig. 4. Effect of removing most of the plastic wake around the crack faces [29].

is certainly questionable because actual K_{op} values were not measured.

Hertzberg et al. [31] tested 7 mm thick Al-Cu-0.7Si Al alloy and 9 mm thick 4340 steel specimens, and studied the effect of increasing K_{op} by using 50, 75, and 100 μm thick shims between the crack faces. For the Al alloy, K_{op} increased from 13% to 30%, 50%, and 93% of K_{max}, while FCG rates reduced by a factor of 1.2, 2.7, and 4.7. However, if really caused by ΔK_{eff}, FCG rates should reduce by a factor 16, 27, and 800, respectively, not by the values reported by the authors. Similar results were found for the 4340 steel. Therefore, FCG rate estimates based on measured K_{op} lead to *non-conservative* predictions for these tests. This experimental evidence indicates that, contrary to Elber's hypothesis, crack closure affects, but does not eliminate fatigue damage below K_{op}. However, the authors did not question Elber's idea, and assigned this difference to a possible error induced by the crack closure measurement method, an extensometer at the crack mouth, doubting in this way their own data. Far field crack closure measurements are sometimes questioned because they could yield lower values than near field measurements [12,32], but many authors do not report any significant differences when measuring K_{op} by both techniques [18,19,33]. In fact, near field K_{op} measurements could even induce higher errors due to their high strain gradients.

The same authors also measured FCG rates and K_{op} levels after a compressive UL followed by fixed {ΔK, R} load cycles (Fig. 5). The FCG rate stabilized after a crack increment $\Delta a \cong$ 2–3 mm from the UL point, while K_{op} only stabilized after $\Delta a \cong$ 9–10 mm. So, after a growth $\Delta a \cong 3$ mm, the FCG rate remained essentially constant under *variable* ΔK_{eff}.

Fleck [34] measured FCG rates and K_{op} levels before and after an OL in 3 mm and 24 mm thick specimens of BS4360 50B low strength steel, to grow cracks under plane stress and plane strain under otherwise constant ΔK and R conditions. Extensometers at the crack mouth and strain gages at the specimen back face, as well as at the crack surface 2.5 mm behind the crack tip, were used to measure K_{op}. Fig. 6a presents the measured FCG rates and Fig. 6b the opening loads, indirectly

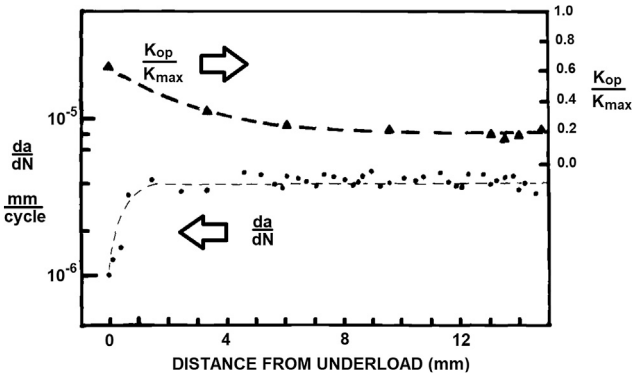

Fig. 5. FCG rate and K_{op} for an Al alloy after a compressive underload [31].

represented by the closure ratio $U = (K_{max} - K_{op})/(K_{max} - K_{min})$. In the 24 mm thick specimens, the opening SIF K_{op} at the surface reduced to values near K_{min} ($U \approx 1$) just after the OL (so with a null crack increment $\Delta a = 0$), but without a proportional increase in FCG rates. For this thick specimen, K_{op} gradually reduced for crack increments between $\Delta a = 2$ and 8 mm, but the corresponding FCG rates kept fairly constant under a variable ΔK_{eff}.

For the thin 3 mm specimens, K_{op} remained constant between $\Delta a = 2$ and 6 mm, but the FCG rate started to increase just before $\Delta a = 4$ mm. Assuming these measurements are coherent, and recalling that Fleck measured the opening loads using three different methods, these data indicate that ΔK_{eff} was not the controlling FCG parameter. However, the author assigns the K_{op} inability to explain the FCG behavior to a "discontinuous closure" behavior. According to him, a residual hump of stretched material would be created by the OL, which would become the point of first contact between the crack surfaces along the subsequent FCG. This material would act like a spring, allowing cyclic displacements ahead of the crack tip below K_{op}. Hence, the SIF range that actually loads the crack tip would be higher than indicated by the K_{op} measurements and, consequently, FCG rates would be higher than predicted by ΔK_{eff}.

Testing 12 mm thick C(T) specimens of A542/2 2.25Cr1Mo steel under plane strain conditions and otherwise constant $\Delta K = 10$ MPa√m and $R = 0.7$ loads, Castro et al. [17] reported significant FCG retardation after a 50% OL ($K_{OL} = 1.5 \cdot K_{max}$), see Fig. 7a. However, due to the high R used in these tests, the crack remained fully open before and after the OL, because $K_{min} > K_{op}$, as the linear compliance measurements prove in Fig. 7b. Since $\Delta K_{eff} = \Delta K$ before and after the OL in these tests, the memory effects cannot be explained by Elber's plasticity induced crack closure PICC [4], simply because there is no crack closure either before or after the OL. Moreover, the authors present many other similar results where the FCG behavior was not controlled by ΔK_{eff} either.

More recently, cracks were grown under plane stress in 2 mm and under plane strain in 30 mm thick specimens of SAE 1020 steel, loaded under constant ΔK and K_{max}, see Fig. 8. During the FCG process, the opening loads K_{op} were frequently measured by redundant near and far field compliance methods [18], and by digital image correlation (DIC) techniques as well in [19]. These independent experimental methods measured near identical K_{op} in all tests. Notice in Fig. 8 that K_{op} continuously reduced as the fatigue cracks advanced, increasing thus the corresponding ΔK_{eff} (*measured*, not inferred), while the FCG rate kept almost constant in all tests. Hence, these results certainly indicate that the FCG behavior was not controlled by ΔK_{eff} in those easily reproducible experiments.

Minimum FCG rates after OL were observed by Davidson and Hudak in 7091-T7E69 Al alloy specimens after crack increments $pz/8 < \Delta a < pz/4$, evidence of delayed FCG retardation according to them [33]. In fact, K_{op} should reduce just after the OLs, which blunt crack tips, locally increasing ΔK_{eff} and accelerating FCG rates, not

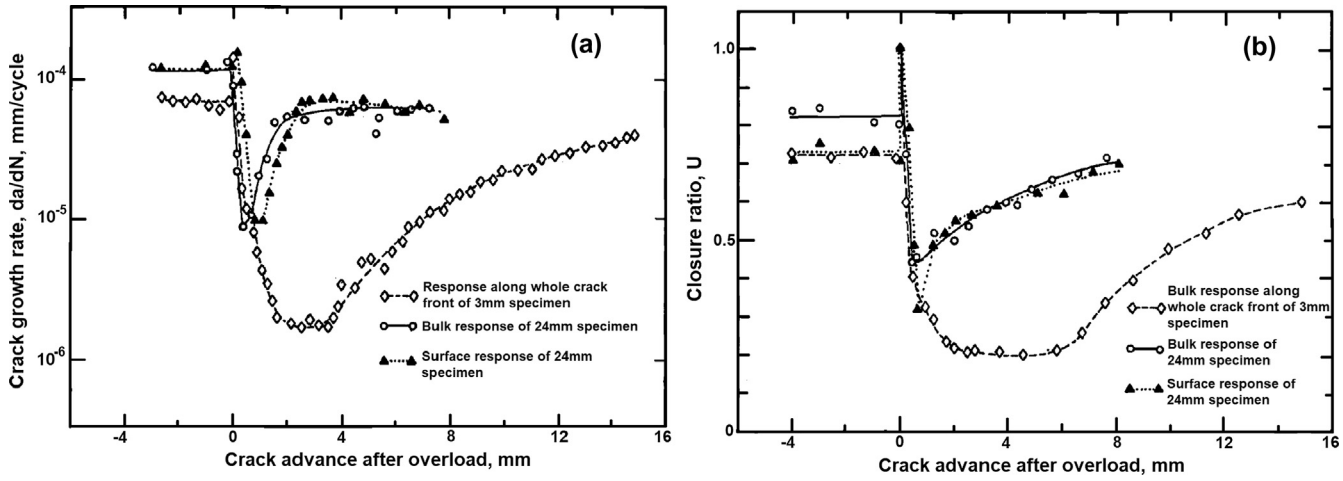

Fig. 6. FCG rate (a) and crack closure (b) measurements [34].

immediately lowering them as shown in that paper. Fig. 9a shows their FCG rates and ΔK_{eff} (measured by SEM techniques) vs. crack increment Δa (positive after the OL), measured before and after an OL ($\Delta K_{OL}/\Delta K = 2.85$). Fig. 9b shows similar results for an OL followed by an UL. Notice in Fig. 9a that even with the increase in ΔK_{eff} observed just after the OL, the corresponding FCG rates reduced immediately.

According to the authors, the residual displacements ahead of the crack tip after an OL is usually tensile and the crack faces remain opened by several millimeters behind its tip. These measurements confirm the cause for the opening load reduction after an overload event. On the other hand, when the OL is followed by an UL, as shown in Fig. 9b, the FCG rate increased about 8 times just after the OL. To correlate this FCG rate increase with ΔK_{eff}, the $da/dN = C\Delta K_{eff}^{m}$ rule exponent should be $m = 5.83$. The authors do not report their m value, but a median estimate for 54 series 7xxx Al alloys is $m = 3.2$ [2]. Fig. 9b also shows a continuous decrease in subsequent ΔK_{eff} values, but with an increase in FCG rates for $\Delta a > 0.1$ mm crack increments. A compressive UL increases the reversibility of the displacements during unloading and decreases the residual displacements ahead of the crack tip with a respective increase of the plastic compressive deformation.

Toyosada and Niwa [35] considered that fatigue cracks can only grow if new plastic strains are induced ahead of their tips, a reasonable idea. They proposed a way to measure the load that tends to initiate the formation of new tensile plastic strains during FCG tests in SM-41B steel 10 mm thick specimens. They showed that SIF ranges associated with FCG thresholds are related to no new cyclic plastic strains and thus to no new damage at the crack tip. They verified as well that FCG rates did not correlate well with the measured ΔK_{eff} for the entire tested range.

Similar tests were conducted by Lang [36]. He measured the minimum SIF needed to propagate fatigue cracks, and claimed that this would occur when the material adjacent to the crack tip becomes free of compressive residual stresses. He verified that this SIF value increases after OLs, and decreases with the reduction of the minimum load during unloading. In FCG tests where an OL is followed by a compressive UL, the SIF reduces with the increase of the modulus of the compressive underload. The SIFs measured by Lang are in accordance with the displacement measurements presented in [33]. These results indicate that FCG is directly related to the interaction between the monotonic and the reverse plastic zones. Since higher compressive residual stresses must be relieved to propagate a crack inside a monotonic plastic zone hypertrophied by an OL, OLs tend to reduce FCG rates and to increase the SIF needed to propagate the crack. On the other hand, ULs after an OL tend to increase the reverse plastic zones, increasing FCG rates and decreasing the SIFs needed to further grow the crack. These hypotheses are coherent with the results presented in [17,33,37].

Data from Chen et al. [15] are particularly interesting. They evaluated the ΔK_{eff} concept in FCG tests of Al specimens keeping $R = 0.3$ fixed and gradually reducing ΔK until reaching the threshold ΔK_{th} (defined by rates da/dN $< 10^{-12}$ m/cycle). At the threshold, the load cycle was $K_{max} = 3$ MPa√m, $K_{min} = 0.9$ MPa√m and the measured opening load was $K_{op} = 2$ MPa√m. After reaching ΔK_{th}, K_{min} was reduced to zero to continue the tests under $R = 0$. This R reduction did not change ΔK_{eff}, but caused a significant increase in FCG rates, as shown in Fig. 10a. Repeated compliance measurements confirm that K_{op} and thus ΔK_{eff} remained constant after the R reduction, see Fig. 10b.

In other words, Fig. 10 shows that the decrease in K_{min} increased ΔK and the FCG rates, but *not* ΔK_{eff}, which remained constant. Hence, these results clearly indicate that the load cycle portion below the opening

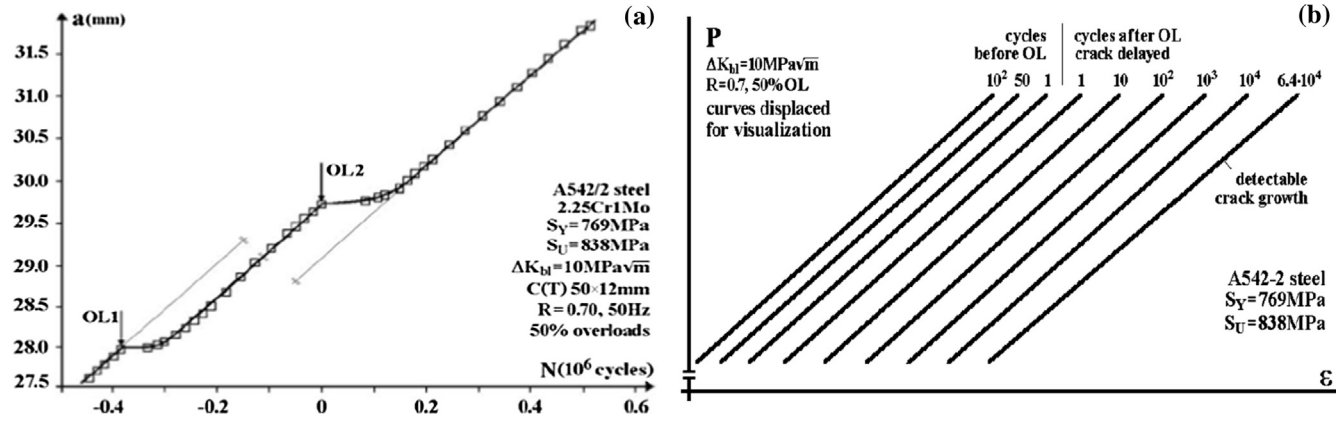

Fig. 7. FCG rate (a) and opening loads (b) results from [17].

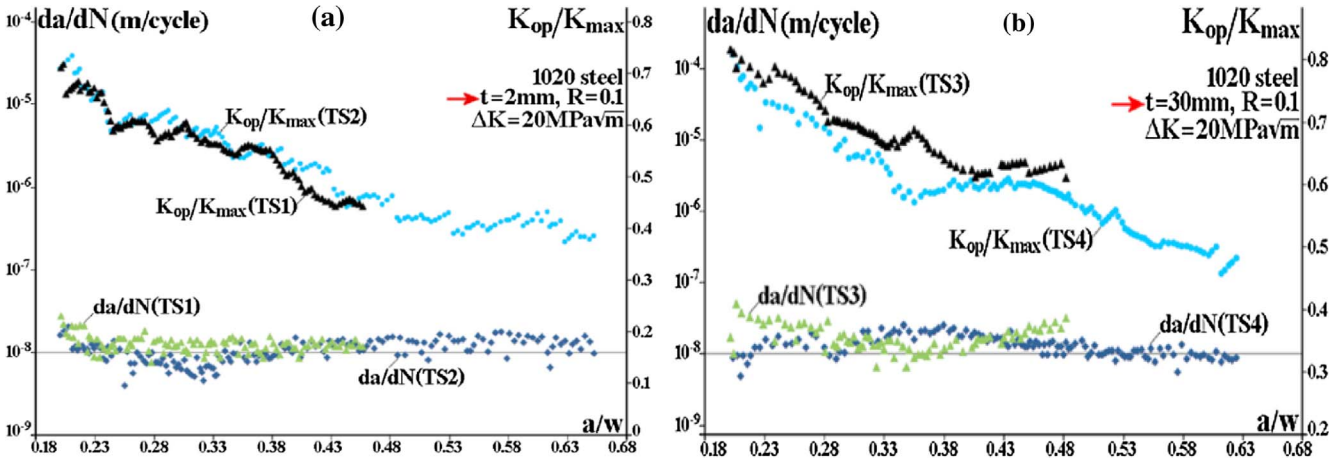

Fig. 8. FCG rate and opening loads for specimens of 2 mm (a) and 30 mm (b) [18].

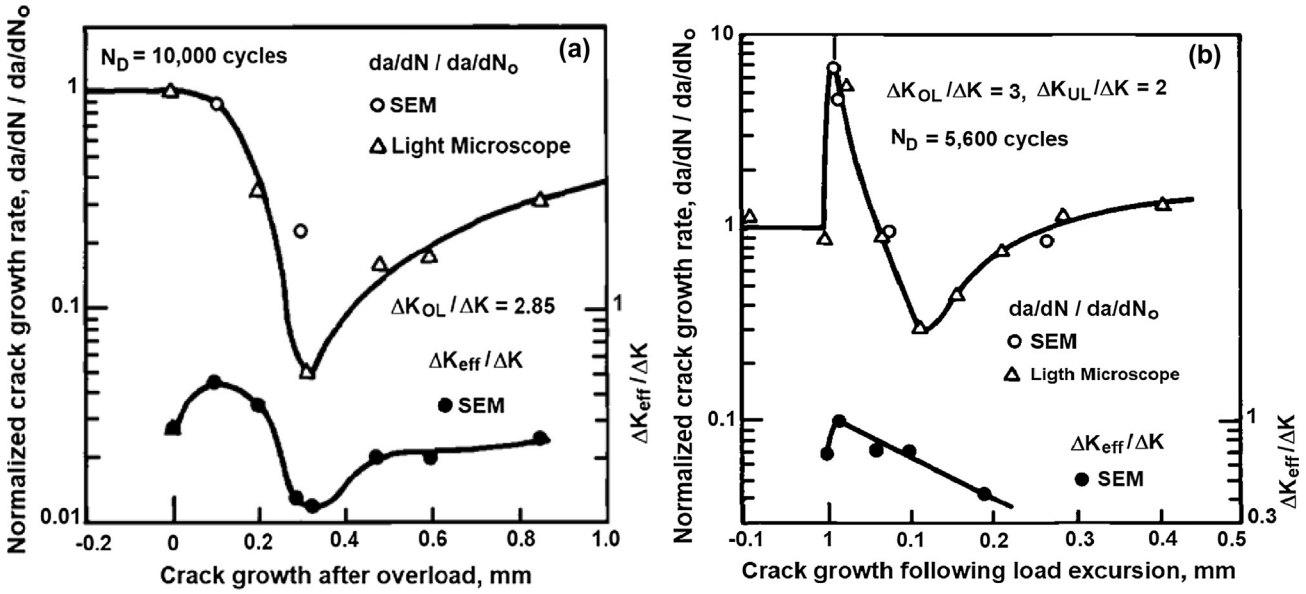

Fig. 9. da/dN and ΔK_{eff}: (a) $\Delta K_{SC}/\Delta K = 2.85$, (b) $\Delta K_{SC}/\Delta K = 3$ followed by $\Delta K_{SubC}/\Delta K = 2$ [33].

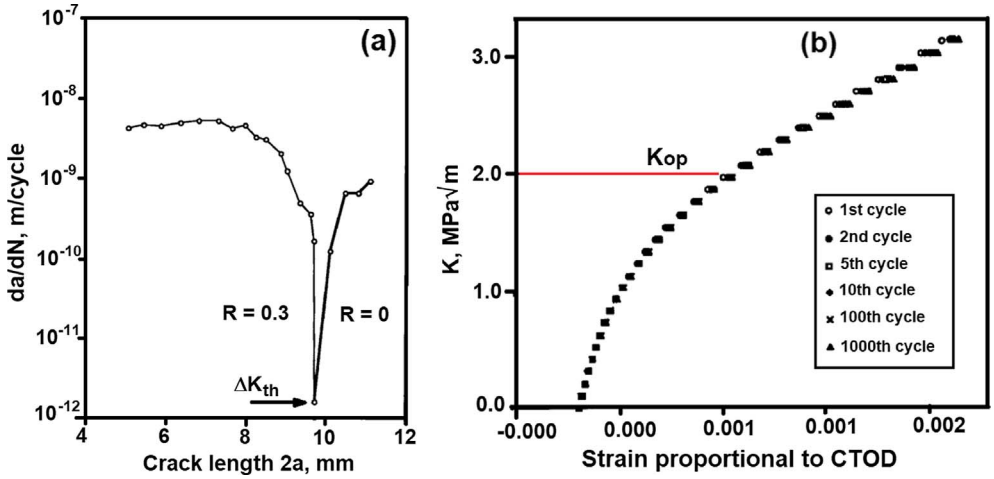

Fig. 10. FCG rate (a) and opening load (b) for a 2024 Al alloy [15].

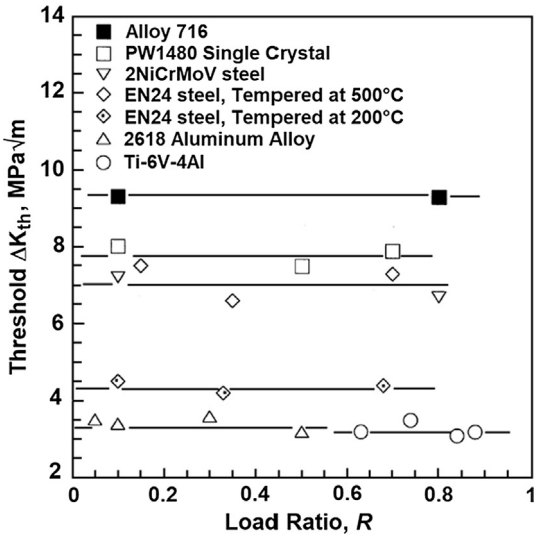

Fig. 11. FCG threshold measurements in vacuum at various *R*-ratios [16].

load contributed to the FCG process, a strong evidence against the "ΔK_{eff} is the FCG driving force" *hypothesis*. Indeed, an arrested crack that resumes growing after an *R* reduction that did not alter ΔK_{eff} is an undisputable evidence of fatigue damage induced below K_{op}. This damage can be related to the increase of the reverse plastic zone size during the unloading cycle part, which increases the plastic strain range ahead of the crack tip.

Other strong evidence presented by Vasudevan et al. [16] seriously questions the actual ΔK_{eff} role in FCG: the *R*-independent FCG thresholds of various alloys tested in high vacuum, see Fig. 11 (which shows data measured by various authors in Al and Ti alloys, steels, Ni superalloys, and even single crystals). If $da/dN = f(\Delta K_{eff})$, then these data would indicate that the effect of plasticity-induced crack closure is either negligible or non-existent in vacuum. However, since vacuum suppresses the effects of the environment, but not of plasticity, how could the measured ΔK_{th} values remain constant over the entire *R* range, if they were caused by Elber's PICC? Vasudevan claims that this set of data indicates that the FCG threshold behavior normally explained in terms of crack closure effects should be, in fact, related to the environment contribution to the FCG process.

In other words, the ΔK_{eff} *hypothesis* assumes the residual ligament is completely shielded from any further fatigue damage below K_{op}. After the crack tip closes under tensile loads, shielding can affect for sure the crack geometry, since its faces should not displace after closed. But the gradual closing of the crack faces may not avoid all further increments of the plastic strain ranges in the residual ligament or the elastoplastic behavior ahead of the crack tip during unloading below K_{op} [37]. In such cases ΔK_{eff} can overestimate the PICC effect and generate non-conservative FCG predictions. This also can possibly be the cause for the many inconsistencies observed when trying to use actually measured crack opening loads (instead of indirect pieces of evidence like the fitting of *da/dN* data) to quantitatively explain some characteristics of the FCG behavior, as discussed above.

Indeed, these data indicate that the behavior of the uncracked ligament ahead of the crack tip can be more important for FCG than the behavior of the plastic wake that encloses the crack faces behind it. They also indicate that crack closure may be a consequence of the FCG behavior, rather than its cause, so that its significance can be overestimated by the ΔK_{eff} hypothesis. Hence, identifying the true fatigue crack driving force is still a most important issue when developing FCG models that can reproduce the physics of memory effects observed under service loadings.

It is well known that fatigue cracks nucleate due to accumulation of plastic strain cycles, and that such cracks do not grow through virgin material. Instead, they grow by cutting material that has already been damaged by the monotonic *pz* and by the reverse or cyclic pz_r plastic zones that always follow their tips. Hence, to assume that the history of plastic strain ranges ahead of the crack tip is the actual mechanical driving force for FCG is at least as reasonable as the ΔK_{eff} hypothesis.

The strain range distribution ahead of the crack tip is much affected by its high stress concentration. At each load cycle, the loading blunts the crack tip eliminating its singularity and forming a *pz* proportional to K^2_{max} (at least under LEFM conditions). The unloading, on the other hand, tends to re-sharp the crack tip and to form a pz_r proportional to ΔK^2. That is why *da/dN* rates correlate well with {ΔK, K_{max}} (or {ΔK, R}) pairs. Moreover, load peaks K_{max} activate monotonic damage mechanisms, like fracture and environmentally assisted cracking [2,14,16], whereas load ranges ΔK drive cyclic damage mechanisms, which may be also affected by the peak loads K_{max}, by the crack opening load K_{op}, and by the residual stresses left ahead of the crack tip. The elastic residual ligament around the predominantly tensile *pz* tend to induce compressive residual stresses, which however can be much affected by the previous loading history [2,38]. In other words, reverse plastic zones pz_r cause direct fatigue damage, whereas monotonic plastic zones *pz* may cause compressive residual stresses that shield the crack tip during FCG. Therefore, the total fatigue damage in each load cycle depends on both the monotonic and the reverse plastic strains, as well as on the residual stress field ahead of the crack tip induced by the previous load history.

This explanation is reasonable, but it does not solve the problem of how model and quantify the plastic strain range distribution ahead of the crack tip. However, it can be used to explain memory effects observed in FCG based on damage accumulated by cyclic plastic strains and on the residual stresses ahead of the crack tip, instead of on ΔK_{eff} arguments [37].

Crack closure may affect the FCG behavior as long as it can affect stress/strain fields and thus the elastoplastic hysteresis loops ahead of the crack tip. Unless supported by direct K_{op} measurements, FCG models cannot assume the material ahead of the crack tip is completely shielded while the tip is not fully open. Hence, residual life predictions made by ΔK_{eff}-based FCG models should be tested by decent K_{op} data and by proper EP loops measurements ahead of the crack tip.

Overloads increase both *pz* and pz_r, as well as the mainly compressive residual stress field and the accumulated fatigue damage ahead of the crack tip. They may also affect the crack tip geometry, inducing crack branching that may further reduce FCG rates by decreasing its local SIFs just after the OLs [39]. All these effects may affect subsequent FCG rates. Initial accelerations observed after some OLs can be related to the increase in damage accumulated by reverse plastic strains, whereas the shielding effect of compressive residual stress fields reduces pz_r and retards FCG rates. After the crack crosses the region affected by the OL, the size of the monotonic and reverse plastic zones, as well as the FCG rate, return to their previous values. This competition can qualitatively explain most memory effects in FCG induced by VAL without the need to assume the ΔK_{eff} hypothesis.

Withers et al. [40] present clear and direct evidence of the compressive residual stress field ahead of the crack tip after an OL. They used X-ray diffraction (XRD) and digital image correlation (DIC) techniques to measure the strain field and to calculate the associated stress field ahead of the crack tip before and after an overload in C(T) specimens of bainitic HY80 steel. Fig. 12(a) shows the stresses at the maximum load and Fig. 12(b) the stresses at the minimum load. The effect of the residual stress field generated by the OL is to reduce the amplitude of the stress at the maximum load (compare in Fig. 12a the stresses at OL-1 and at OL + 40) and by almost the same ratio to reduce the residual stress field at the minimum load (see in Fig. 12b the stress at OL-1 and at OL + 40). These stress fields after the OL confirm the shielding effect induced by compressive residual stresses. Lower monotonic and reverse plastic zones, while the crack is inside the region affected by the previous OL, reduce the cyclic plastic strains and cause

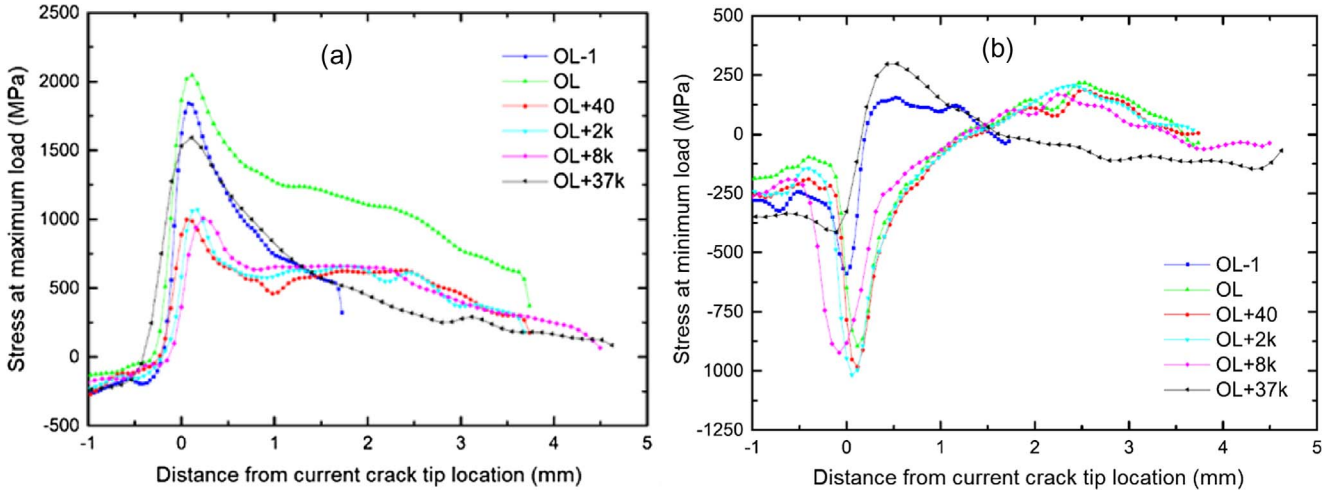

Fig. 12. Stress profile at the maximum load (a) and at the minimum load (b) [40].

retardation in the subsequent FCG rates.

Despite so many serious questions about the ΔK_{eff} hypothesis, it has been used in many FCG models, in particular the strip-yield models (SYM) [5–9] that probably still are the most used to predict FCG under service loads for design proposes, in a wide range of applications. However, the FCG process can also be modeled without assuming ΔK_{eff} is the FCG driving force, supposing it is caused by the cyclic plastic strain history that acts ahead of the crack tip. Moreover, since the simplified SYM mechanics used by most FCG models based on the ΔK_{eff} idea is reasonable, it can also be used to estimate the damage accumulation process ahead of the crack tip, as discussed next.

4. Damage accumulation ahead of the crack tip based on the strip-yield mechanics

SYMs are based on Dugdale-Barenblatt's idea [41,42], modified to leave plastically deformed material around the faces of the advancing fatigue crack [5–9]. Plastic zone sizes *pz* and surface displacements are estimated by the superposition of two linear elastic solutions: a cracked plate loaded by (i) a remote uniform nominal tensile stress σ_n, and (ii) a uniform distributed stress σ applied over crack surface segments. The numerical model developed by Newman [6] for a M(T) specimen uses rigid-perfectly bar elements whose displacements are described by

$$V_i = \sigma_n f(x_i) - \sum_{j=1}^{n} \sigma_j \cdot g(x_i, x_j) \tag{1}$$

The influence functions $f(x_i)$ and $g(x_i, x_j)$ used in Eq. (1) are related to the plate geometry and to its width correction, as expressed in Eqs. (2)–(4). In those equations: x is the bar element central position, d is the fictitious crack (actual crack plus *pz* size), W is the half-width of the cracked plate, η is a stress state correction (η = 0 for plane stress and η = ν for plane strain condition), E is Young's modulus, the parameters B_1, B_2, b_1, and b_2 are calculated by Eqs. (5)–(7).

$$f(x_i) = [2(1-\eta^2)/E]\sqrt{(d^2 - x_i^2)\sec(\pi d/2W)} \tag{2}$$

$$g(x_i, x_j) = G(x_i, x_j) + G(-x_i, x_j) \tag{3}$$

$$G(x_i, x_j) = \frac{2(1-\eta^2)}{E}\left\{(b_2 - x_i)\cdot\cosh^{-1}\left(\frac{d^2 - b_2 x_i}{d|b_2 - x_i|}\right) - (b_1 - x_i)\cdot\cosh^{-1}\left(\frac{d^2 - b_1 x_i}{d|b_1 - x_i|}\right) + \sqrt{d^2 - x_i^2}\cdot[\sin^{-1}(b_2/d) - \sin^{-1}(b_1/d)]\cdot\left[\frac{\sin^{-1}B_2 - \sin^{-1}B_1}{\sin^{-1}(b_2/d) - \sin^{-1}(b_1/d)}\right]\cdot\sqrt{\sec\left(\frac{\pi d}{2W}\right)}\right\} \tag{4}$$

$$B_k = \sin(\pi b_k/2W)/\sin(\pi d/2W) \tag{5}$$

$$b_1 = x_j - w_j \tag{6}$$

$$b_2 = x_j + w_j \tag{7}$$

Eq. (1) is used to calculate the bar element plastic deformation and also the contact stress required to estimate the crack opening stress [6,43]. Newman's original model also uses a fracture mechanics rule to calculate FCG based on the ΔK_{eff} hypothesis [6,43]. A SYM algorithm was developed and implemented in this work following these ideas, as described in [27].

Another way to model the FCG process is to assume that fatigue cracks grow by a gradual damage accumulation process in the uncracked ligament ahead of their tips, caused by the cyclic elastoplastic (EP) stress and strains histories that act there [17,20–24]. These critical-damage models (CDM) divide the ligament into a set of small volume elements (VE) and assume that the fatigue cracks grow by sequentially breaking the element adjacent to their tips when it reaches the critical damage the material can sustain. The CDM originally proposed in [23,24] uses only physically-based hypotheses and does not need any data-fitting parameter. It uses a shifted HRR strain-stress field to estimate the plastic strain ranges ahead of the crack tip, recognizing crack tip blunting to remove its singularity, and estimates FCG rates in the three phases of Paris curve using a McEvily-like FCG curve. These CDMs were later generalized to deal with VAL conditions [17]. Its formulation is detailed in [27], where its predictions are compared with those from the SYM, and with the predictions from a new mixed model based on the combination of CDM and SYM concepts as well.

In the CD/SY mixed model proposed in [27], the deformation field generated by SYM procedures, see Eq. (1), is used to calculate the strain field ahead of the crack tip and to replace the shifted HRR field of the original CDM. The FCG rate is again calculated by using a McEvily-like FCG rule. In summary, three models are described and their predictions are compared and analyzed in [27]: (i) the original strip-yield model (SYM), (ii) the original critical damage model based on a shifted HRR field (CDM) and (iii) the mixed critical damage/strip yield model (SY-CDM).

This paper main objective is to propose a significant improvement for the SY-CDM, to avoid its need to assume a suitable, but somehow arbitrary FCG rule. This new version can simulate the three phases of typical FCG curves directly from fatigue damage accumulation induced by cyclic plastic strain histories ahead of the crack tip, without the need for any other artificial tricks or arbitrary data-fitting constants. This modified strip-yield critical-damage combined model (named SY-CDMmod) estimates FCG increments in a cycle-by-cycle basis considering a gradual damage accumulation process and possible crack

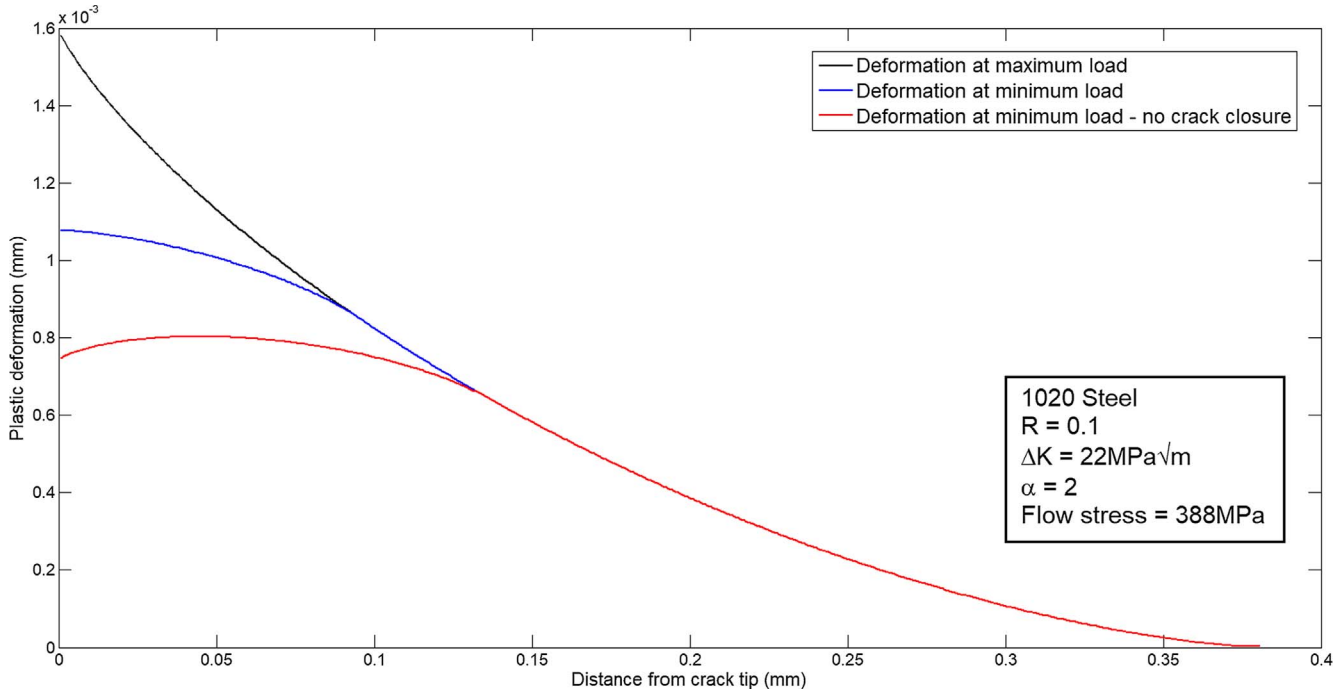

Fig. 13. Plastic displacement ahead of the crack tip from SY-CDMmod.

closure effects on the cyclic strain field ahead of the crack tip. So, it combines Newman's strip-yield ideas [6,43] to calculate the strain field ahead of the crack tip with CDM routines developed by Castro et al. [23,24], considering contact element effects during unloading, but not assuming ΔK_{eff} is the FCG driving force. For FCG under constant SIFs $\{\Delta K, K_{max}\}$ (fixed plastic zone sizes) or stresses $\{\Delta\sigma, \sigma_{max}\}$ (slowly growing plastic zone sizes), no memory effects occur during FCG. Plastic deformations at maximum (σ_{max}) and minimum (σ_{min}) applied stresses are calculated by Eqs. (8) and (9), obtained from Eq. (1), where S_F is the flow stress, α is the triaxiality constraint factor (which varies from plane stress to plane strain limit conditions), and n_{pz} is the number of bar elements inside the plastic zone. The element stress at minimum applied load, σ_j in Eq. (2), is calculated by solving the equation system Eq. (10) using a Gauss-Seidel iteration process with added restraints [6].

$$L_{max}(i) = \sigma_{max} \cdot f(x_i) - \sum_{j=1}^{npz} \alpha \cdot S_F \cdot g(x_i, x_j) \tag{8}$$

$$L_{min}(i) = \sigma_{min} \cdot f(x_i) - \sum_{j=1}^{n} \sigma_j \cdot g(x_i, x_j) \tag{9}$$

$$(\sigma_i)_I = [Sf_i - L_{max,i} - \sum_{j=1}^{i-1} (\sigma_j)_I g_{ij} - \sum_{j=i+1}^{n} (\sigma_j)_{I-1} g_{ij}]/g_{ii} \tag{10}$$

Fig. 13 shows the plastic deformation ahead of the crack tip estimated by the SY-CDMmod at maximum and minimum loads, using Eqs. (8) and (9) in two conditions: (i) considering the elements at the crack surface and (ii) assuming no plastic deformation around the crack surfaces, thus no crack closure. Like in the SYMs, the broken elements are kept along the crack surfaces and are used to consider possible crack closure effects in the cyclic strain field ahead of the crack tip. This figure also shows how the contact of the crack surfaces (crack closure) affects their values. Hence, the FCG rates calculated by the proposed SY-CDMmod are affected (but not controlled) by crack closure (which reduces the reverse plastic zone size, and the plastic strain ranges inside it as well).

The SY-CDMmod divides the monotonic plastic zone *pz* into small rigid-plastic bar elements, assumed analogous to tiny εN specimens. Due to the simplified material behavior assumed by the SYM mechanics (rigid-perfectly-plastic, neglecting elastic and strain-hardening effects), damage occurs only into the reverse plastic zone pz_r. The damage calculation precision depends on the strain gradient inside the pz_r, so it may need more than the 20 elements used in the original SYM (which works well with fewer variable element widths because it is less sensitive to its strain gradient). Fatigue damage must be calculated, accumulated, and stored in a cycle-by-cycle basis. To reduce numerical errors, all bar elements have the same initial width. SYMs estimate plastic deformation and stresses at the center of each bar element. This original characteristic is kept in the proposed SY-CDMmod. Crack increments can be located between two adjacent bar elements, as a consequence of the critical damage value (usually assumed as 1). So, an interpolation routine is needed to locate them and to correctly store the damage information in each one of its 400 bar elements inside the monotonic plastic zone (assuming $n_{pz} = 400$ is enough, as discussed further on).

Since original SYM procedures calculate peak and residual plastic *deformations* at each bar element, they must be adapted to generate the strain field needed by the proposed SY-CDMmod. This problem is solved using a formulation proposed by Rice that estimates cyclic strains for tensile cracks based on crack opening displacements [44], assuming the crack root radii are the current crack opening displacements resulting from the prior deformation history. Rice's solution assumes an idealized elastic-perfectly plastic material and proportional plastic flow, i.e. plastic strain tensor components that remain proportional in all bar elements inside *pz*. It also assumes that prior to any loading the crack tip radius is null, so that further crack tip blunting must result from plastic straining. Rice's formulation is properly modified to consider the calculated plastic strain of the various bar elements ahead of the crack tip as in Eq. (11). The deformation L_{max} and L_{min} of the i^{th} element inside the *pz* are calculated at the maximum and minimum applied stresses by Eqs. (8) and (9). The positions of the elements starting from the crack tip, $x_{ct}(i)$, are located at the center of each bar element.

$$\Delta\varepsilon_y = log\,[(2L_{max}(i) + x_{ct}(i))/(2L_{min}(i) + x_{ct}(i))] \tag{11}$$

The SY-CDMmod proposed here eliminates the need the original

CDM and the SY-CDM [27] have to suppose $da/dN \times \Delta K$ curves described by a suitable (but nevertheless arbitrary) McEvily-like rule by assuming two new hypotheses, based only on εN principles and on the physics of the FCG process. The first assumes that if a fatigue limit exists, there is a limit strain range below which the crack does not grow, which is directly related to the SIF threshold range ΔK_{th}. So, an applied load range equivalent to the threshold induces a strain range ($\Delta\varepsilon y_{,th}$) that does not cause damage to the crack. The second hypothesis assumes the crack becomes unstable at a maximum plastic strain related to the critical stress intensity factor, i.e. to the material toughness. The critical plastic strain ($\varepsilon_{y,cr}$), associated with the stress that would induce the critical SIF, is the maximum plastic strain the cracked body can sustain before breaking. Using Eq. (11), $\Delta\varepsilon y_{,th}$, and $\varepsilon_{y,cr}$, the effective plastic strain range ($\Delta\varepsilon y_{,eff}$) is then calculated by

$$\Delta\varepsilon_{y,eff} = [\Delta\varepsilon_y - \Delta\varepsilon_{y,th}]\cdot[\varepsilon_{y,cr}/(\varepsilon_{y,cr} - \varepsilon_{y,max})] \quad (12)$$

The effective plastic strain range $\Delta\varepsilon_{y,eff}$ that acts at the center of each element ahead of the crack tip can be correlated with the number of cycles $N(i)$ that would be required to break that element if that range was kept constant. $N(i)$ can be calculated from the plastic part of Coffin-Manson's rule using Eq. (13), or from the SWT rule using Eq. (14):

$$N(i) = (1/2)(\Delta\varepsilon_{y,eff}(i)/2\varepsilon_c)^{1/c} \quad (13)$$

$$N(i) = (1/2)(\sigma_{max}(i)\cdot\Delta\varepsilon_{y,eff}(i)/2\sigma_c\varepsilon_c)^{1/(b+c)} \quad (14)$$

Please notice that the effective strain range used in Eqs. (13) and (14) depends on material properties (threshold and critical strains), but not on ΔK_{eff}. Notice as well that this SY-CDMmod formulation only considers the plastic part of the strain range, because strain ranges calculated from SYM-estimated deformations assume a rigid-perfectly-plastic material ahead of the crack tip, neglecting their elastic components. The fatigue damage at each bar element, evaluated by linear Palmgren-Miner's rule Eq. (15) (or by any other suitable rule) is accumulated at every load cycle. Crack increments are assumed equal to the distance where the accumulated damage reaches 1.0. The stress σ_{max} from Eq. (14) is calculated considering tri-axial restrictions near the crack tip ($\sigma_{max} = \alpha\cdot S_F$).

$$D(i) = 1/N(i) \quad (15)$$

When contact stresses at crack surface are considered, a crack growth rate transient behavior appears at the initial phase of the numerical simulation even under constant SIF ranges, due to the gradual formation of the crack wake. Therefore, the width of the bar elements cannot be assumed equal to the crack increments like in [24]. The proposed SY-CDMmod model is able to deal with VAL or even with the transient behavior at the initial simulation phase, changing the width of the first and of the last elements inside the plastic zone. Therefore, although not considered in this work, which deals only with simulations of $da/dN \times \Delta K$ curves measured under fixed {ΔK, K_{max}} conditions, this CDM is versatile and can deal with VAL as well, following ideas outlined in [27].

The SY-CDMmod calculates strains, stresses and fatigue damage at the central position of each bar element, and the crack increment (Δa) progresses up to a position where the accumulated damage reaches a critical value. Normally this position is found through an interpolation between two adjacent elements, while defining the residual ligament rl of the element where the crack tip stops after a load cycle as depicted in Fig. 14, where a half load cycle is schematically illustrated. Notice that the bar element just ahead of the crack tip is called element 1, the next unbroken element is called 2, and so on, while the first broken element is called n, the second is (n–1), etc.

Since the number of bar elements is unchanged to keep their widths sum equal to the pz size, the broken part of the partially broken element in a cycle is added to the last element n_{pz} located at the pz frontier in the next cycle. Hence, this model uses only two bar elements with variable width inside the plastic zone, the first and the last one. The

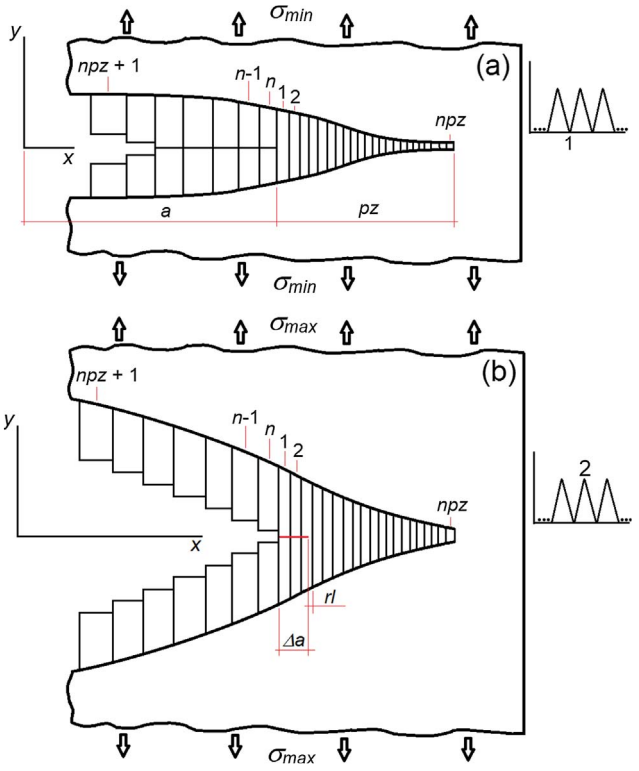

Fig. 14. Schematic of the bar elements' behavior during the tensile part of a load cycle.

accumulated damage in the central position of the new first element is calculated by linear interpolation. The whole algorithm is implemented in a homemade Matlab code following the flow diagram depicted in Fig. 15.

It is interesting to mention that the Unigrow model proposed in [25] also estimates FCG based on damage accumulation, assuming the SIF due to compressive residual stress is the mechanism that induces load order effects. However, although both the proposed SY-CDMmod and the Unigrow are based on similar principles, they have many important diferences. The Unigrow requires a fracture mechanics based FCG (Kujwaski) rule to predict FCG considering ΔK and K_{max} as the fatigue crack driving forces. Moreover, to calculate SIFs induced by compressive residual stress fields and to calibrate its FCG rule, it uses many strong hypotheses that may be questionable, as futher discussed elsewhere [2,27].

Anyway, one of the main differences between the two models is in the domain discretization ahead of the crack tip: while the proposed SY-CDMmod uses a large number of elements, the first and last with variable width, Unigrow arbitrarily supposes that the element width is not only constant, but a material property as well, called the elementary material block size ρ^*. Moreover, its crack tip radius is assumed constant and equal to ρ^*, instead of estimating it as a function, for example, of the CTOD. This ρ^* is used to calculate the stress concentration factor of the opened crack of length a, while the closed crack, which always has a SIF equal to zero, is assumed to behave as a circular hole with radius ρ^*. Unigrow estimates the stress field ahead of the crack tip using Creager and Paris' linear elastic (LE) solution for a blunt notch. This LE field is used with the cyclic Ramberg-Osgood curve and Neuber's strain concentration rule to calculate the EP stress and strain fields. Finally, Unigrow estimates the life of the first element ahead of the crack tip N^* using the Smith-Watson-Topper (SWT) parameter, and then the consequent FCG rate as $da/dN = \rho^*/N^*$. In fact, this hypothesis is used to calibrate the ρ^* parameter from da/dN data measured under the same loading conditions used to calculate the material block life N^*. Therefore, Unigrow cannot claim to be a true predictive model, since it requires FCG measurements to model FCG rates.

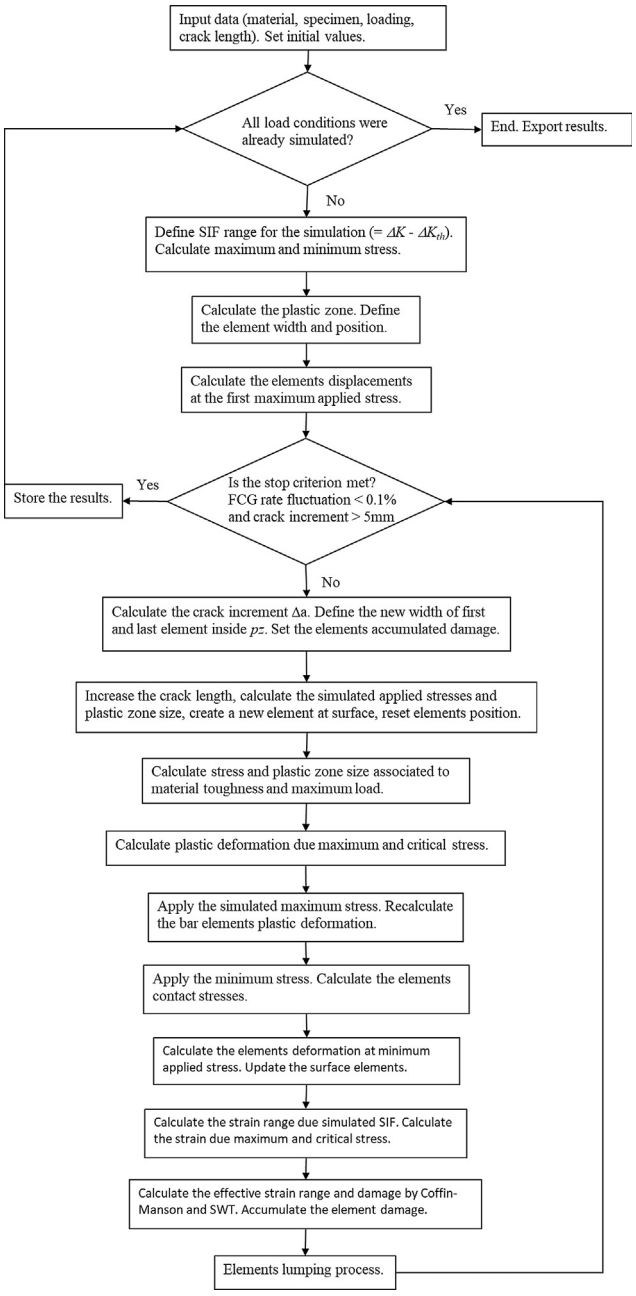

Fig. 15. Flow diagram of the modified strip-yield critical damage model.

The proposed SY-CDMmod, on the other hand, uses the SYM formulation to calculate the plastic strain field ahead of the crack tip. Moreover, unlike the Unigrow, it considers the contact of the elements along the crack wake. It can use SWT or any other εN rule to calculate damage at each load cycle, but the consequent crack increment is defined by the length where the damage reaches the unit value. In this sense, it is a true predictive model for FCG rates, since it does not require any previous calibration, or any data-fitting parameter for that matter. So, there are many differences between these two models; a more detailed analysis is found in [2,27].

5. Results and discussion

These four models (SYM, CDM, SY-CDM, and SY-CDMmod) are compared with experimental $da/dN \times \Delta K$ data measured at $R = 0.1$ and $R = 0.7$ for two materials, a 7075-T6 Al alloy and a 1020 low carbon steel, following standard ASTM E647 procedures as described elsewhere [27]. Material properties used for FCG rate predictions with the SY-CDMmod are listed in Table 1. Applied loads (σ_{max}, σ_{min}) are recalculated at each cycle to keep ΔK constant. Since the SYM formulation was developed for a center cracked plate and the data was measured in C(T) specimens, the K-analogy is used to define the applied stress as explained in [43]. Since the tests were made under plane strain conditions, a constraint factor $\alpha = 2$ is adopted for both materials. Since the SY-CDM and the SY-CDMmod use strains calculated from SYM procedures, it is necessary to define this parameter. For each material and load condition, the simulation stopped only after reaching a FCG rate fluctuation lower than 0.1% with a minimal crack increment of 5 mm.

Figs. 16–19 show the measured $da/dN \times \Delta K$ points and the curves predicted by six models. First, by the original CDM based on Creager and Paris (C&P). Second, by the original SYM assuming a plastic constraint $\alpha = 3$ for 7075 and $\alpha = 2$ for 1020 condition A, as explained in [27]. Third, by two SY-CDMs (SY-CDM C&M and SY-CDM SWT) proposed in [27]. Finally, by two SY-CDMmod proposed here (SY-CDMmod C&M and SY-CDMmod SWT). As explained before, the experimental data points are for a 7075-Al alloy and for a 1020 steel, and all SYM-CDM curves are predicted from the εN damage induced by the cyclic strain fields estimated by strip-yield procedures using Coffin-Manson or SWT εN rules, using only the plastic part of those εN rules. Once again, this simplification is needed for a fair comparison, since the numerical procedures used in the SYMs discretize the pz ahead of the crack tip assuming rigid-perfectly-plastic VE elements. Recall that Coffin-Manson does not recognize mean or maximum stress effects, whereas SWT does. Recall as well that the SYM-CDMmod proposed here does not need to use a previously chosen da/dN rule, due to the two limiting strains introduced in this new model.

Notice in Fig. 16 that the da/dN curves estimated by the SY-CDM based on Coffin-Manson (C&M) and by the original C&P CDM proposed in [24] are essentially equal. Both estimates are reasonable for $R = 0.1$, albeit not as good for $R = 0.7$ (Fig. 17). The original SYM curve (estimated assuming $\alpha = 3$) describes better the data points measured at $R = 0.7$ (Fig. 17), but generates non-conservative predictions for lower ΔK at $R = 0.1$ (Fig. 16). Critical damage FCG rate estimates based on SWT are higher than the estimates based on Coffin-Manson for both R-ratios, as expected. The model proposed here that uses a Coffin-Manson damage calculation (SY-CDMmod C&M) yielded the best estimates for $R = 0.1$ (Fig. 16) and had a reasonable performance (similar to the original SYM) for $R = 0.7$ (Fig. 17).

The SYM-CDMmod had in particular a better performance at the higher ΔK ranges, where the original models systematically estimated FCG rates higher than the measured data. It is important to emphasize that the SY-CDMmod does not need to assume a pre-defined FCG curve. It does not need to use any adjustable data-fitting constant either. It only needs εN properties and suitable strain limits associated to the FCG threshold and the toughness of the material. The original CDM [24] and the SY-CDM need to assume a pre-chosen McEvily-type $da/dN \times \Delta K$ curve, whose single adjustable parameter can however be calculated by εN procedures. The former also needs to assume a displaced HRR field to describe the strain field ahead of the crack tip and to eliminate the (unreal) crack tip singularity, as explained in [27]. The original SYM, on the other hand, assumes a ΔK_{eff}-based Forman-Newman FCG curve with four adjustable data-fitting parameters [45].

Therefore, the reasonable performance of the CDMs certainly is not a coincidence, since their FCG predictions are entirely based on measured εN properties and use no adjustable data-fitting parameters. In fact, when compared to SYM estimates based on ΔK_{eff} concepts and on a FCG rule that needs 4 adjustable parameters, not to mention the constraint factor α that in practice is frequently used as a 5th data-fitting parameter, the CDM performance could be even qualified as quite impressive for such a simple model. Even though a reasonable data-fitting cannot be considered as proof of the SY-CDMmod validity, it at least indicates that the CDM hypotheses are reasonable.

Table 1
Material properties used at the SY-CDMmod simulations.

Material	S_Y (MPa)	S_U (MPa)	s_c (MPa)	e_c	b	c	K_{IC} (MPa√m)	ΔK_{th} (MPa√m)	
								$R = 0.1$	$R = 0.7$
7075-T6	498	576	709	0.12	−0.056	−0.75	25.4	3.4	2.9
1020	285	491	815	0.25	−0.114	−0.54	277	11.6	7.5

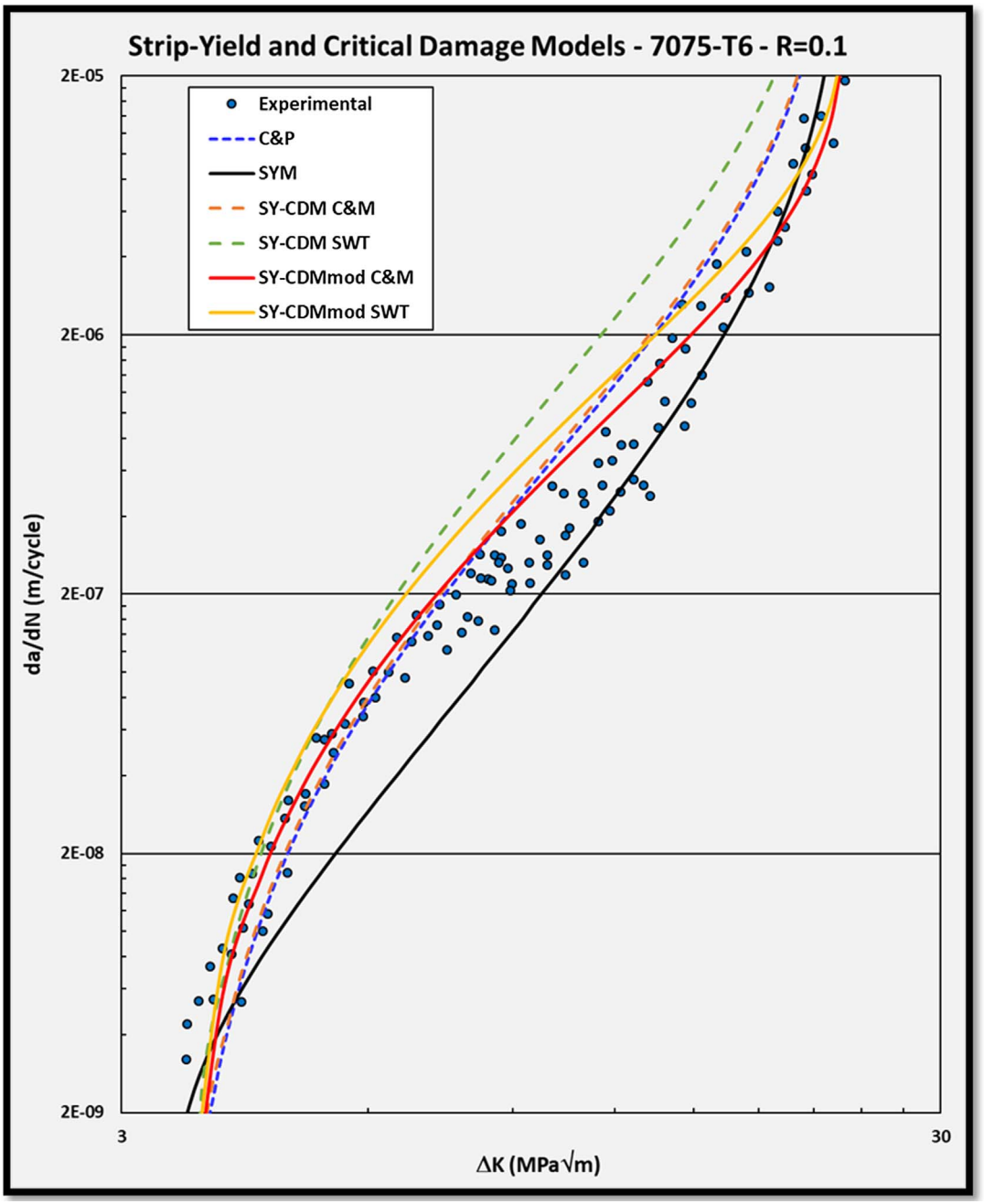

Fig. 16. Strip-yield and critical damage models for the Al 7075-T6 at $R = 0.1$.

The 1020 steel results are shown in Figs. 18 and 19. The original CDM based on a Creager and Paris shift of the HRR field origin (see [27] for details) reproduced quite well the data trend, but yielded slightly non-conservative FCG estimates at $R = 0.1$ (Fig. 18). For $R = 0.7$ (Fig. 19) it presented a still better performance. The original SYM had a similar performance at $R = 0.1$, but instead generated slightly conservative predictions, which deviated from the data at low ΔK values (Fig. 18). For $R = 0.7$ its predictions were too conservative, see Fig. 19. The SY-CDMmod based on C&M generated quite reasonable predictions for $R = 0.7$ (Fig. 19), but for $R = 0.1$ they were maybe too conservative (Fig. 18). The other models yielded too conservative predictions for both R-ratios. The conservative results probably are due to the 1020 steel's higher sensitivity to strain hardening effects compared to the 7075 Al alloy, since the algorithm uses rigid-perfectly-plastic elements

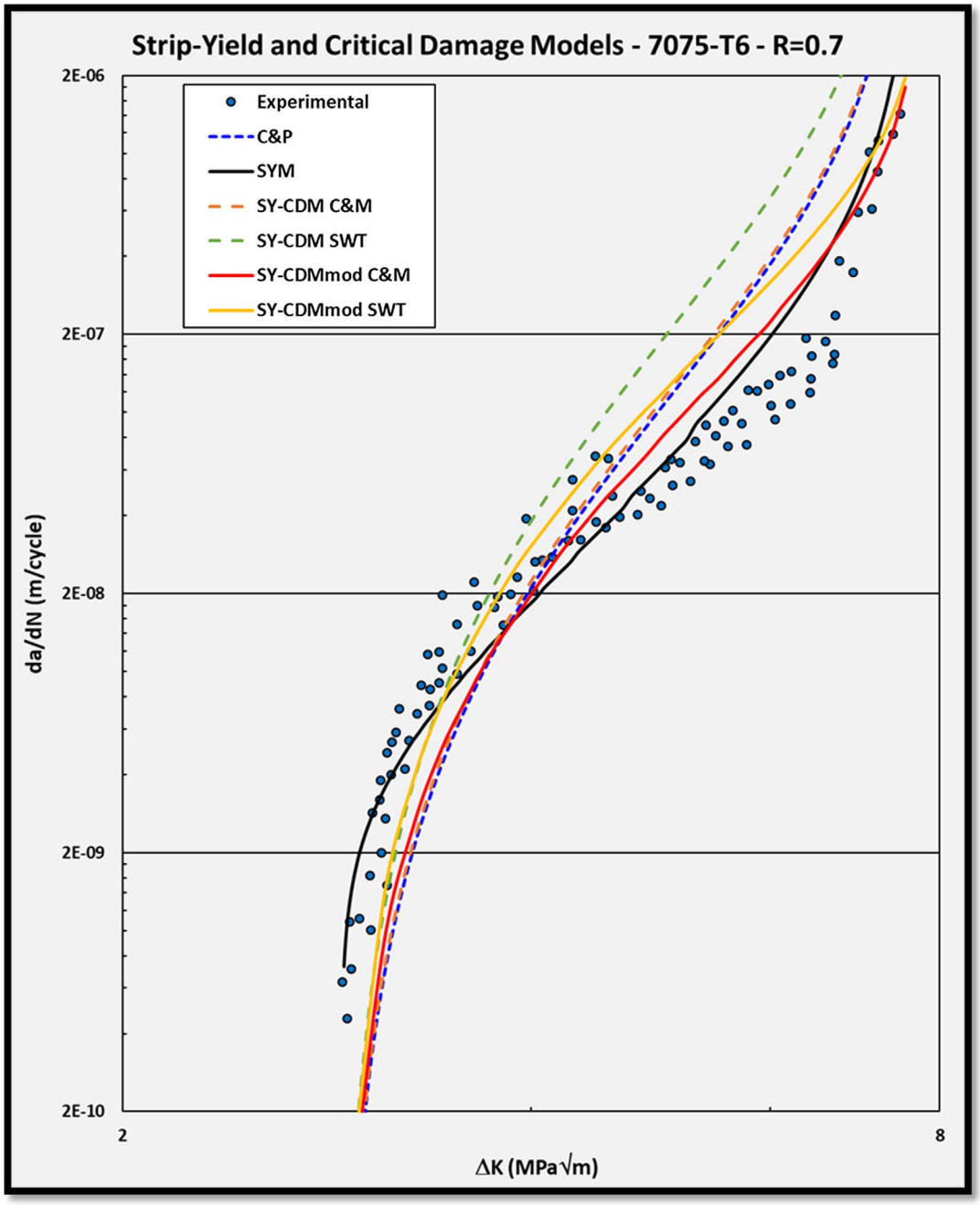

Fig. 17. Strip-yield and critical damage models for the Al 7075-T6 at $R = 0.7$.

(the strain hardening exponents are 0.09 for the 7075 and 0.18 for the 1020 [27]). This material stress-strain simplification comes from the formulation of the strip-yield model adopted to generate the strain fields of the SY-CDMmod model.

Two facts resulting from this exercise must be emphasized. First, their FCG estimates are quite reasonable, an indication that their simplified ideas about the mechanics of the FCG process probably are reasonable as well. This is as an indication that the procedures used in these simple models are at least coherent, a reassuring evidence. However, the second fact is still more interesting, since it could not be anticipated. The results presented in Figs. 16–19 show that FCG rates estimated by opposing ideas about the actual crack driving forces can yield similarly reasonable results. Moreover, when the SYM and the CDM techniques are properly combined, they also generate reasonable predictions. This does not mean that these methods are equivalent. Indeed, while the CDM FCG rate estimates require only measurable εN properties and need no data-fitting parameters, the SYM estimates use at least four data-fitting parameters to achieve similar results.

Finally, besides the many details already discussed when presenting the modeling techniques and their performance compared to the measured data, both here and in the companion article [27], an additional philosophical point must be emphasized as well. Although not related to the modeling procedures, it is as important as the mechanics for the quest of finding better ways to model FCG problems. The results presented in both articles indicate that the ideas behind the modeling procedures seem reasonable, but they indicate as well that a good description of some experimental data *cannot* be claimed as a conclusive proof of any model suitability, let alone of its prevalence. What is really important when discussing such conflicting ideas is to clearly identify which set of properly measured experimental data any given FCG model *cannot* describe well. Since after so many years still there is no consensus about such questions, not even about which are the true fatigue

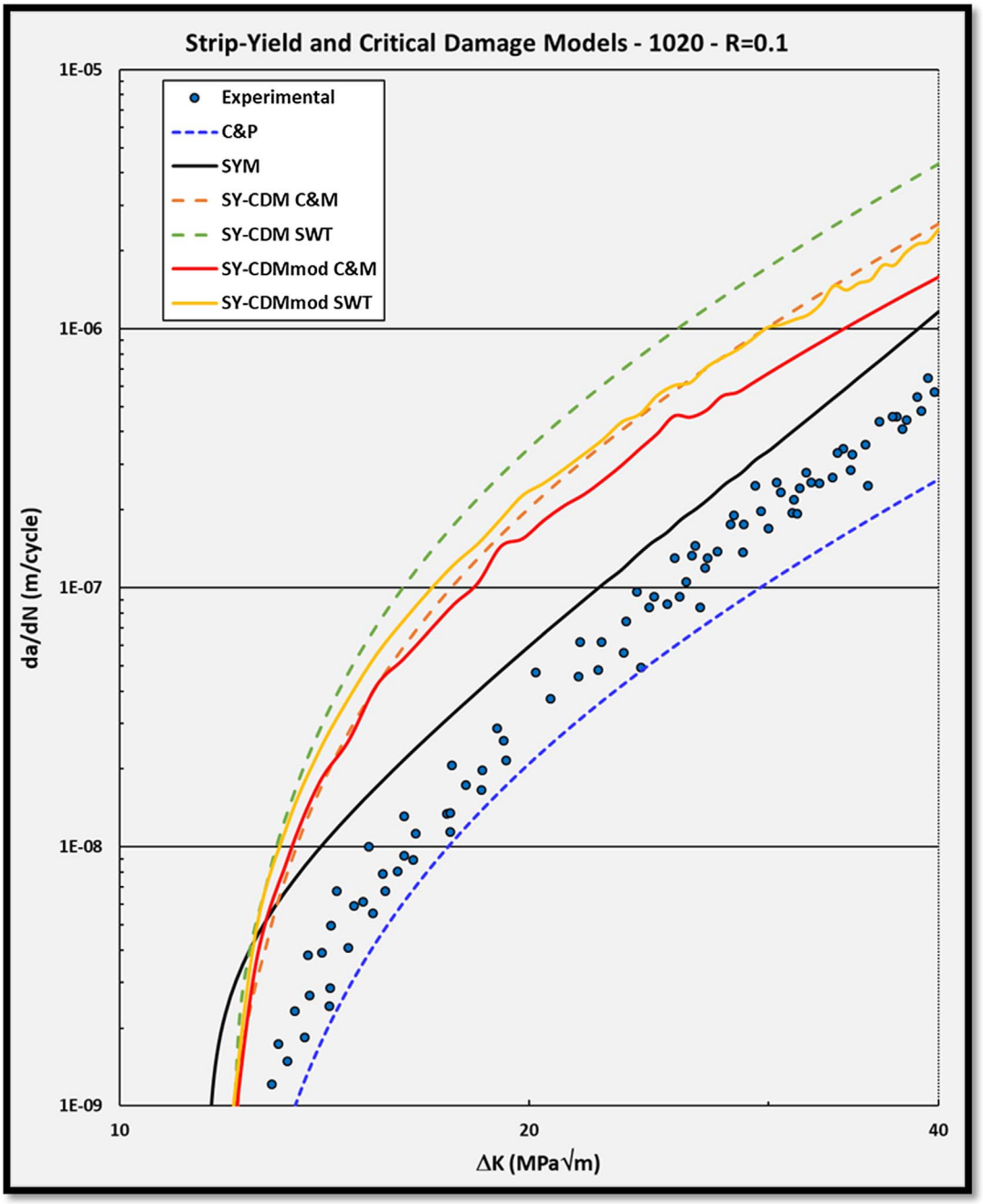

Fig. 18. Strip-yield and critical damage models for the 1020 steel at $R = 0.1$.

crack driving forces, the authors hope this relatively straightforward modeling exercise can contribute at least to avoid the radical opinions that are still too common in this field.

6. Some comments on the SY-CDMmod numerical robustness

In the CDMs presented in [24], the bar element width is directly related to the crack increments. It works well for constant amplitude loading, but requires adaptations to deal with VAL conditions. For those cases, an algorithm that assumes all bar elements ahead of the crack tip have constant width, but allows the existence of a partially cracked element at the crack tip, was proposed in [26]. Under VAL, the number of bar elements inside the plastic zone may be varied at every load cycle in order to keep the width of the elements equal to the model resolution, e.g. 10^{-7} m (this value can, of course, be adjusted by the user). Hence, fatigue damage can be calculated at these tiny element borders.

However, the combined SY-CDMs developed to predict FCG rates based on the combination between strip-yield and critical damage procedures, both here and in [27], calculate damage at the center of the bar elements, since this is the way displacements and stresses are calculated in the original SYM. Moreover, to keep the width of the bar elements constant, the plastic zone ahead of the crack tip must be discretized in a relatively large number of elements (400 elements in the SY-CDMmod presented above). This high number of elements is not arbitrary. It was chosen after a few convergence tests for two reasons. First, due to possible effects of the element width in the model resolution, since the strain gradient ahead of the crack tip is high, and second due to the computational facility of accumulating damage in this way.

However, the original SYM discretizes the plastic zone ahead of the crack tip (as well as the plastic wake left around the crack faces), and achieves convergence using much fewer variable-width bar elements

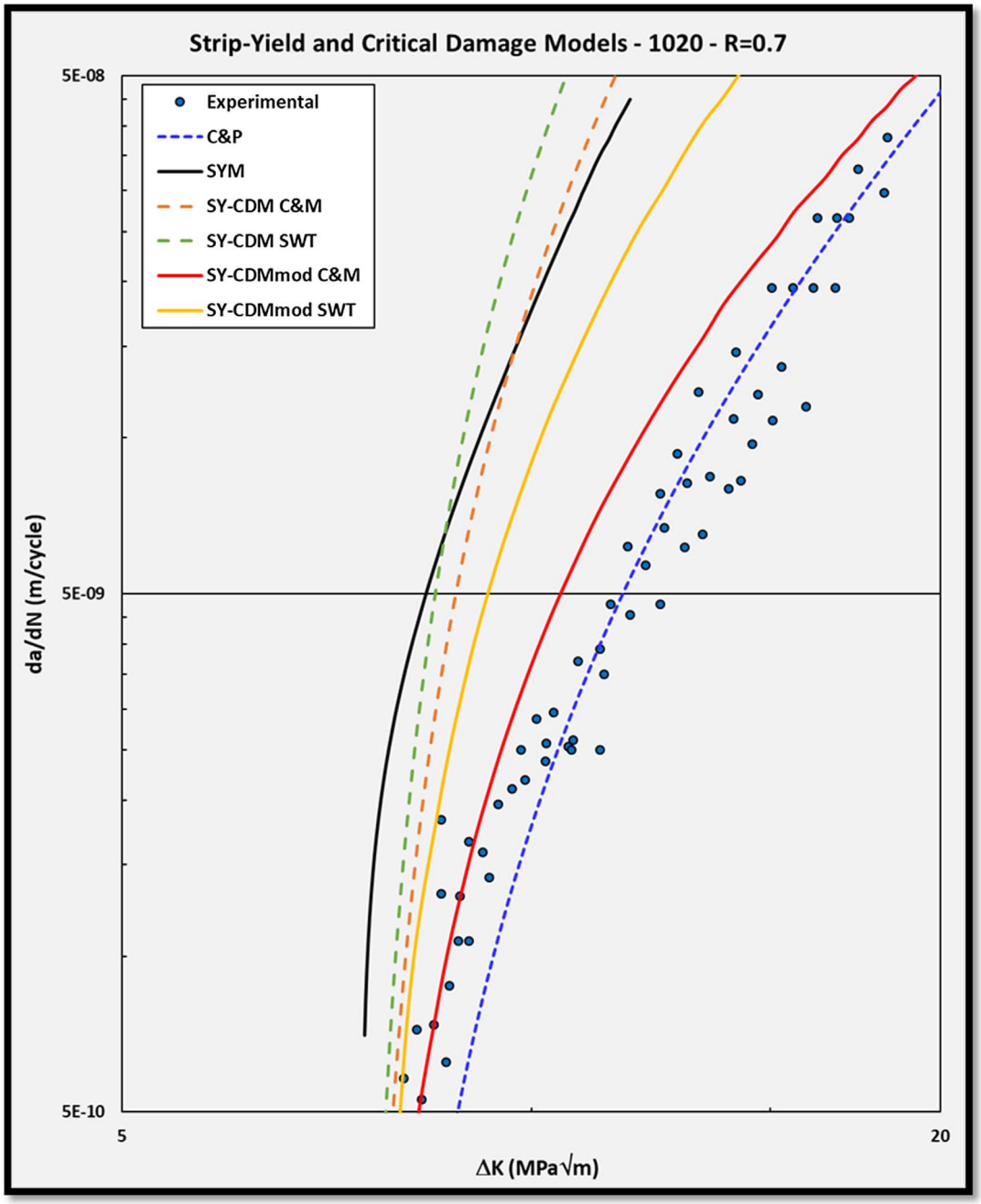

Fig. 19. Strip-yield and critical damage models for the 1020 steel at $R = 0.7$.

[6]. Therefore, it is worth to test this idea in the SY-CDMmod algorithm too. To do so, the algorithm has to be properly modified to deal with variable-width bar elements. However, to keep its good resolution while reducing computer costs, the bar elements near the crack tip must be chosen with a very small width. Two conditions are then tested and compared with the predictions made by the SY-CDMmod C&M using 400 fixed-width bar elements, as discussed and presented above. First, 20 variable-width bar elements have been used like in the original SYM, maintaining the ratio between their widths and the plastic zone size as follows: 0.005, 0.005, 0.005, 0.005, 0.01, 0.01, 0.02, 0.02, 0.03, 0.03, 0.045, 0.045, 0.06, 0.06, 0.075, 0.075, 0.1, 0.1, 0.15, 0.15. Second, 30 variable-width bar elements were used with the following width-to-plastic-zone-size ratios: 0.001, 0.001, 0.001, 0.001, 0.001, 0.001, 0.001, 0.001, 0.002, 0.003, 0.004, 0.005, 0.008, 0.011, 0.014, 0.018, 0.022, 0.026, 0.03, 0.034, 0.039, 0.044, 0.049, 0.054, 0.062, 0.07, 0.078, 0.095, 0.12, 0.204. Figs. 20 and 21 present the results of the FCG rate curves predicted by each method for the 7075 Al alloy and 1020 steel, respectively, using the Coffin-Manson CDM.

It is important to point out that using bar elements with variable widths has a few consequences. Among them, it is necessary to implement a routine that accumulates fatigue damage using some kind of interpolation inside the elements. This interpolation is needed because the strain gradient inside the bar elements may be significant, thus cannot be neglected. A simple linear interpolation was used to generate the curves presented in Figs. 20 and 21.

For the SY-CDMmod with fixed-width bar elements, all elements have initially the same width equal to $pz/400 = 0.0025 \cdot pz$ (except for the first and last elements, which, as explained above, may have different values depending on the point that reaches the critical damage in the previous load cycle). For the model with 20 variable-width bar elements, the first element width is equal to $0.01 \cdot pz$, whereas for the model with 30 elements the first element width is $0.002 \cdot pz$. Figs. 20 and

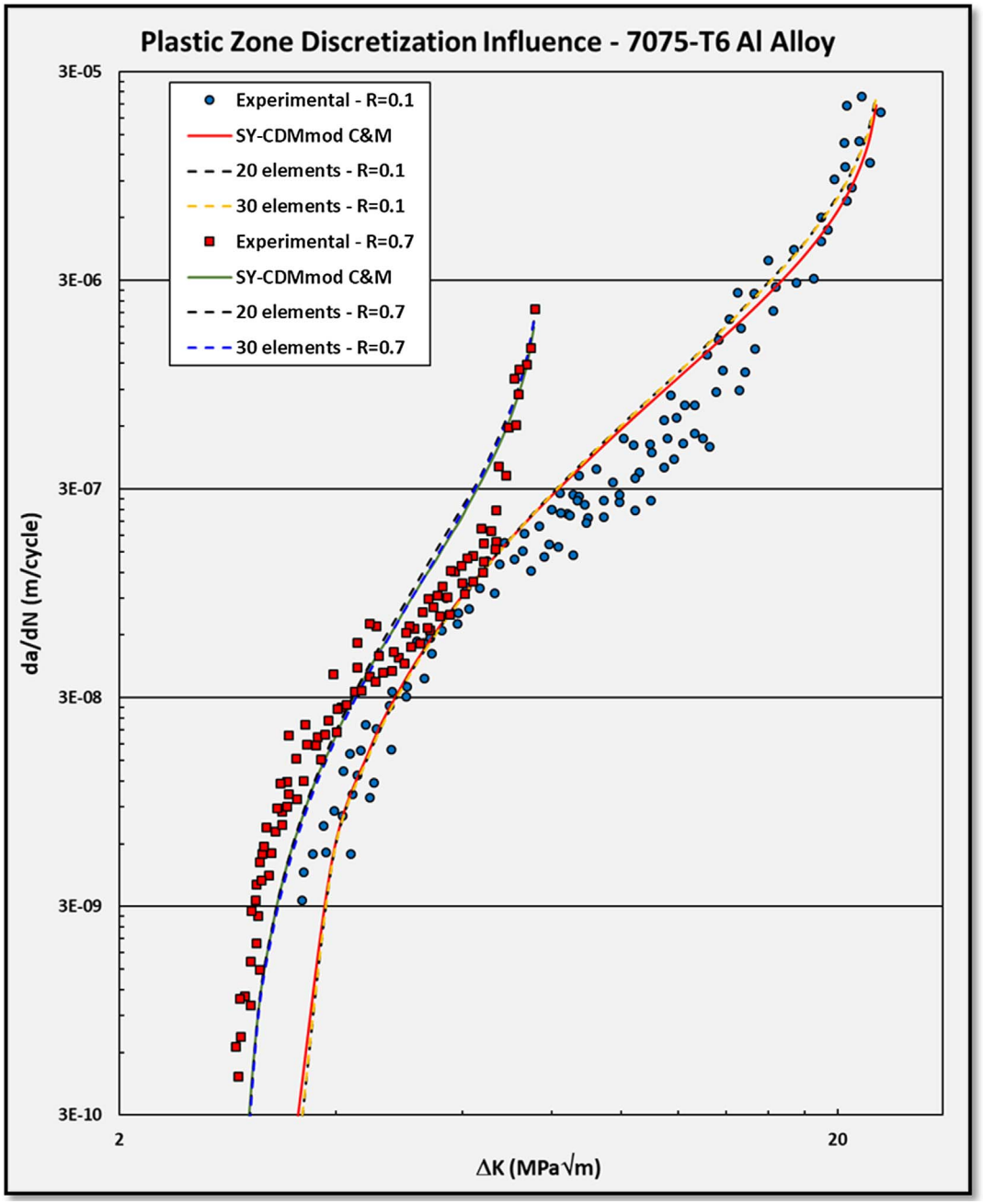

Fig. 20. Plastic zone discretization influence for the 7075 Al alloy.

21 indicate that the predictions of the SY-CDMmod are not too sensitive to the number of variable-width bar elements ahead of the crack tip. Indeed, the FCG curves predicted by the models with 20 and 30 elements are equally satisfactory, mainly for the 7075 Al alloy, where no relevant difference is found with respect to the curve estimated using 400 fixed-width elements. The largest differences are observed for the 1020 steel with $R = 0.7$, where in the worst case the models with 20 and 30 elements estimated FCG rates higher than the fixed-width SY-CDMmod by 32% and 68%, respectively. This is probably due to the 1020 steel high strain hardening characteristic, which tends to increase the error of a model that does not properly consider this effect. The reduction of the number of elements ahead of the crack tip from 400 to 30 and 20 decreased computer time by a factor of about 25 (in average from 800 s to 30 s for each load level, with the calculations made in a common laptop). This interesting feature will further explored when dealing with VAL in future papers.

7. Conclusion

FCG models based on critical damage and on strip-yield/ΔK_{eff} ideas are proposed and used to estimate $da/dN \times \Delta K$ curves of two materials tested under two very different R-ratios. These models are based on contradicting hypotheses about the actual cause for the FCG behavior. Whereas the SYMs assume FCG is primarily driven by ΔK_{eff}, so that it depends on the interference between the plastic wakes left behind the crack tip along the crack surfaces, the CDMs suppose fatigue cracks propagate by sequentially breaking volume elements ahead of the crack tip, because they accumulate all the fatigue damage they could sustain. Moreover, combined SYM/CDM models are proposed by joining the SYM mechanics with the CDM ideas about the causes for the FCG process. In particular, a new modified SYM/CDM model is proposed here to eliminate the need to assume a McEvily-like rule to model the FCG behavior. Using a limit strain range related to the threshold stress

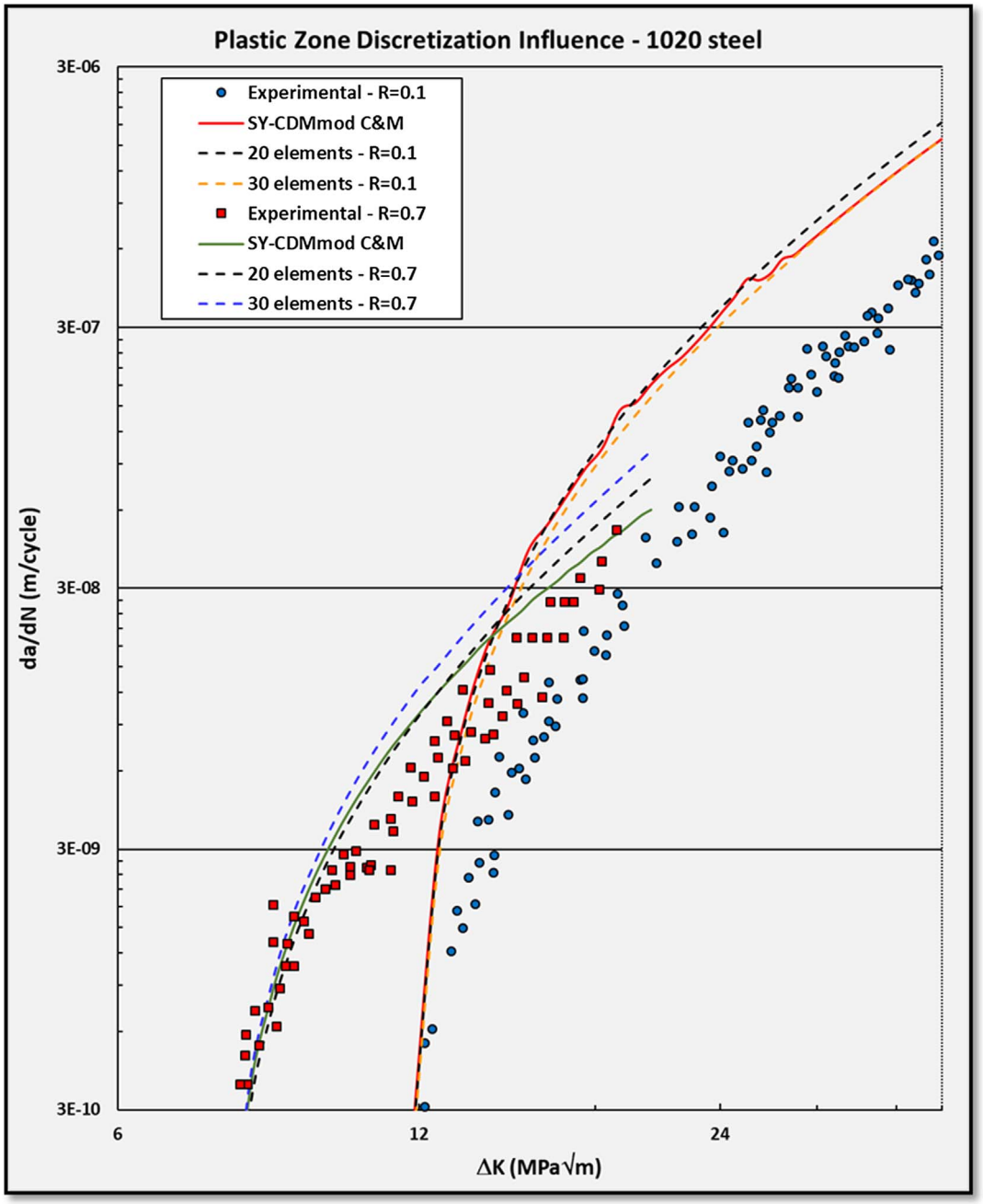

Fig. 21. Plastic zone discretization influence for the 1020 steel.

intensity factor range, and a critical plastic strain related to the critical stress intensity factor, the results of the proposed SY-CDMmod are improved compared to the SY-CDM, which needs to use a pre-defined FCG rule based on Fracture Mechanics principles. The FCG predictions generated by all models studied here are compared against properly measured 7075-T6 Al alloy and 1020 AISI steel FCG data, whose $da/dN \times \Delta K$ curves were experimentally obtained following standard ASTM E647 procedures. The εN properties of such materials, used by the CDMs, have been measured by standard ASTM E606 procedures. Moreover, both the FCG and the crack initiation properties were measured in coupons machined from the same material lot, to avoid any inconsistency in the data. The reasonable performance of the predictions indicates that, although apparently contradictory, such models are not incompatible. It also indicates that the good fitting of some properly obtained data set is not enough to prove which one is the best.

References

[1] Paris PC, Erdogan F. A critical analysis of crack propagation laws. J Basic Eng 1963;85:528–34.
[2] Castro JTP, Meggiolaro MA. Fatigue Design Techniques, vol. 3: Crack Propagation, Temperature and Statistical Effects. CreateSpace; 2016.
[3] Elber W. Fatigue crack closure under cyclic tension. Eng Fract Mech 1970;2:37–45.
[4] Elber W. The significance of fatigue crack closure. Damage Tolerance in Aircraft Structures, ASTM STP 486:230-242, 1971.
[5] Dill HD; Saff CR. Spectrum crack growth prediction method based on crack surface displacement and contact analyses. Fatigue Crack Growth under Spectrum Loads, ASTM STP 595:306-319; 1976.
[6] Newman JC. A crack-closure model for predicting fatigue crack growth under aircraft spectrum loading. Methods and Models for Predicting Fatigue Crack Growth under Random Loading, ASTM STP 748:53-84; 1981.
[7] de Koning AU; Liefting G. Analysis of crack opening behavior by application of a discretized strip yield model. Mechanics of fatigue crack closure, ASTM STP 982:437-458; 1988.
[8] Wang GS, Blom AF. A strip model for fatigue crack growth predictions under general load conditions. Eng Fract Mech 1991;40:507–33.

[9] Beretta S, Carboni M. A strip-yield algorithm for the analysis of closure evaluation near the crack tip. Eng Fract Mech 2005;72:1222–37.
[10] Skorupa M. Load interaction effects during fatigue crack growth under variable amplitude loading – a literature review. Part I: empirical trends. Fatigue Fract Eng Mater Struct 1998;21:987–1006.
[11] Skorupa M. Load interaction effects during fatigue crack growth under variable amplitude loading – a literature review. Part II: qualitative interpretation. Fatigue Fract Eng Mater Struct 1999;22:905–26.
[12] Kemp PMJ. Fatigue crack closure – a review. Royal Aerospace Stablishment: TR90046; 1990.
[13] Williams JJ, Yazzie KE, Padilla E, Chawla N, Xiao X, de Carlo F. Understanding fatigue crack growth in aluminum alloys by in situ X-ray synchrotron tomography. Int J Fatigue 2013;57:79–85.
[14] Vasudevan AK, Sadananda K, Louat N. A review of crack closure, fatigue crack threshold and related phenomena. Mater Sci Eng 1994;188A:1–22.
[15] Chen DL, Weiss B, Stickler R. The effective fatigue threshold: significance of the loading cycle below the crack opening load. Int J Fatigue 1994;16:485–91.
[16] Vasudevan AK, Sadananda K, Holtz RL. Analysis of vacuum fatigue crack growth results and its implications. Int J Fatigue 2005;27:1519–29.
[17] Castro JTP, Meggiolaro MA, Miranda ACO. Singular and non-singular approaches for predicting fatigue crack growth behavior. Int J Fatigue 2005;27:1366–88.
[18] Castro JTP, Meggiolaro MA, González JAO. Can ΔK_{eff} be assumed as the driving force for fatigue crack growth? Frattura ed Integrità Strutturale 2015;33:97–104.
[19] Castro JTP, González JAO, Meggiolaro MA, González GLG, Freire JLF. Some questions about assuming ΔKeff as the sole FCG driving force. Submitted to Int J Fatigue; 2016.
[20] Majumdar S, Morrow JD. Correlation between fatigue crack propagation and low cycle fatigue properties. Fracture toughness slow-stable cracking, ASTM STP 559:159-182; 1974.
[21] Schwalbe KH. Comparison of several fatigue crack propagation laws with experimental results. Eng Fract Mech 1974;6:325–41.
[22] Glinka G. A notch stress-strain analysis approach to fatigue crack growth. Eng Fract Mech 1985;21:245–61.
[23] Castro JTP, Kenedi PP. Prediction of fatigue crack growth rates departing from Coffin-Manson concepts. J Braz Soc Mech Sci Eng 17;1995:292–303, (in Portuguese).
[24] Durán JAR, Castro JTP, Payão Filho JC. Fatigue crack propagation prediction by cyclic plasticity damage accumulation models. Fatigue Fract Eng Mater Struct 2003;26:137–50.
[25] Noroozi AH, Glinka G, Lambert S. A study of the stress ratio effects on fatigue crack growth using the unified two-parameters fatigue crack growth driving force. Int J Fatigue 2007;29:1616–34.
[26] Castro JTP, Meggiolaro MA, Miranda ACO. Fatigue crack growth predictions based on damage accumulation calculations ahead of the crack tip. Comput Mat Sci 2009;46:115–23.
[27] Ferreira SE, Castro JTP, Meggiolaro MA. Using the strip-yield mechanics to model fatigue crack growth by damage accumulation ahead of the crack tip. Int J Fatigue 2017;103:557–75.
[28] Kujwaski D. ΔK_{eff} parameter under re-examination. Int J Fatigue 2003;25:793–800.
[29] James MN, Knott JF. An assessment of crack closure and the extent of the short crack regime in Q1N (HY80) steel. Fatigue Fract Eng Mater Struct 1985;8:177–91.
[30] von Euw EFJ, Hertzberg RW, Roberts R. Delay effects in fatigue crack propagation. ASTM STP: stress analysis and growth of cracks – Proceedings of the 1971 National Symposium on Fracture Mechanics, Part I:230–259; 1972.
[31] Hertzberg RW, Newton CH, Jaccard R. Crack closure: correlation and confusion. ASTM STP 1988;982:139–48.
[32] Ward-Close CM, Blom AF, Ritchie RO. Mechanisms associated with transient fatigue crack growth under variable-amplitude loading: an experimental and numerical study. Eng Fract Mech 1989;32:613–38.
[33] Davidson DL, Hudak Jr SJ. Alterations in crack-tip deformation during variable-amplitude fatigue crack growth. ASTM STP 945: fracture Mechanics. In: Eighteenth Symposium 934–954, 1988.
[34] Fleck NA. Influence of stress state on crack growth retardation. ASTM STP 1988;924:157–83.
[35] Toyosada M, Niwa T. The significance of RPG load for fatigue crack propagation and the development of a compliance measuring system. Int J Fract 1994;67:217–30.
[36] Lang M. Description of load interaction effects by the ΔK_{eff} concept. ASTM STP 1999;1343:207–23.
[37] Silva FS. Fatigue crack propagation after overloading and underloading at negative stress ratios. Int J Fatigue 2007;29:1757–71.
[38] Wang GS. The plasticity aspect of fatigue crack growth. Eng Fracture Mech 1993;46(6):909–30.
[39] Miranda ACO, Meggiolaro MA, Castro JTP, Martha LF. Crack retardation equations for the propagation of branched fatigue cracks. Int J Fatigue 2005;27:1398–407.
[40] Withers PJ, Crespo PL, Mostafavi M, Steuwer A, Kelleher JF, Buslaps T. 2D mapping of plane stress crack-tip fields following an overload. Frattura ed Integrità Strutturale 2015;33:151–8.
[41] Dugdale DS. Yielding of sheets containing slits. J Mech Phys Solids 1960;8:100–4.
[42] Barenblatt GI. The mathematical theory of equilibrium cracks in brittle fracture. Adv Appl Mech 1962;7:55–192.
[43] Newman JC. FASTRAN II: a fatigue crack growth structural analysis program, NASA Technical Memorandum 104159, LRC Hampton; 1992.
[44] Rice JR. Mechanics of crack tip deformation and extension by fatigue. Fatigue crack propagation, ASTM STP 415:247-311; 1967.
[45] NASGRO – fracture mechanics and fatigue crack growth analysis software, reference manual, version 4.02; 2002.